2013-12-11

Nonlinear Spectroscopic Investigation of Adsorption to C-18 Model Stationary Phase

Anthony D. Peterson
Brigham Young University - Provo

Nonlinear Spectroscopic Investigation of Adsorption to C-18 Model Stationary Phase

Anthony D. Peterson

A thesis submitted to the faculty of
Brigham Young University
in partial fulfillment of the requirements for the degree of

Master of Science

Steven R. Goates, Chair
James E. Patterson
Paul B. Farnsworth
Marcus T. Cicerone

Department of Chemistry and Biochemistry

Brigham Young University

December 2013

ABSTRACT

Nonlinear Spectroscopic Investigation of Adsorption to
C-18 Model Stationary Phase

Anthony D. Peterson
Department of Chemistry and Biochemistry, BYU
Master of Science

Reversed-phase liquid chromatography (RPLC) is a commonly used separation technique in chemistry. Nevertheless, the mechanistic interactions at the molecular level among the eluent, analyte, and the stationary phase are not fully understood. Because of this limited understanding, optimization of the separation must be done experimentally. Learning more about molecular interactions should aid in improving separations. We are currently using second-harmonic generation (SHG) spectroscopy to investigate how analytes adsorb to the surface. SHG is a spectroscopic technique that produces signal only at places of non-isotropic symmetry; this typically occurs at surfaces. SHG can be used to produce surface isotherms of test analytes adsorbed to a model C18 stationary phase surface. Fitting these isotherms with a Langmuir model produces an adsorption equilibrium constant. However, the equilibrium constant can only be accurately determined if the true bulk concentration is known; this thesis describes an approach to ensure this. The equilibrium constant relates to Gibbs free energy and is the start to obtaining other thermodynamic information. The long equilibration times of analytes with the stationary phase observed in this study emphasize the importance of both thermodynamic information and kinetic values for understanding retention. Once equilibrium constants and other parameters are accurately obtained, this information can be used to improve predictions and calculations from numerical models.

Keywords: reversed-phase liquid chromatography, RPLC, C-18, second harmonic generation, SHG, surface isotherms, adsorption, PAH, pyrene

ACKNOWLEDGMENTS

I have enjoyed my collegiate experience at Brigham Young University and I would first like to thank the institution for accepting my application for both my undergraduate work as well as for graduate school. I have enjoyed learning in a school that maintains the same high standards that I believe in. I would also like to thank all the professors that have helped me over the years. Most especially I would like to thank Dr. Goates, Dr. Patterson, Dr. Farnsworth, and Dr. Cicerone of my committee for believing in me and for their help with my project. I would also like to thank Dr. Asplund for his willingness to assist me with my project even though he was not on my committee. I cannot thank all the professors enough for all the assistance, encouragement, and support they have given to me.

I would also like to thank Krytal Sly and Dr. John Conboy from the University of Utah for the help they granted me when my project was not working. I appreciate their willingness to allow me to use their system for a day to collect some data that I could use to compare against the data I collected. Without their help, I do not believe my project would have succeeded.

Finally, I want to thank my family and extended family for the help and support and prayers that have gone my way. And most importantly I would like to thank Katie, my wife, for being very understanding as I worked long hours collecting data and working on my project. She has been more help and encouragement than she knows. My wife and daughter, Hannah, have been the best motivation and encouragement that I could have ever asked for.

Table of Contents

Chapter 1

Introduction to RPLC

1.1 RPLC

Reversed-phase liquid chromatography (RPLC) is the principle method used to separate mixtures of organic material;[1] between 80% and 90% of all analytical separations incorporate the use of RPLC.[2] RPLC can be applied to a wide variety of fields, and although it is quite commonly used in analytical chemistry and biochemistry, it is also becoming increasingly used in pharmacology and food science. The importance of RPLC can be seen by the amount of research that has gone into gaining a deeper understanding of the mechanisms of separation that occur on the RPLC column; each year between 1991 and 2012 over 1000 articles related to RPLC were published.

The separation properties of RPLC result from molecules interacting with a nonpolar stationary phase and a polar mobile phase. In some cases, the stationary phase has chains of up to 30 carbon atoms attached to silica particles;[3] however, the most commonly used length is 18 carbons.[4-7] At first glance, the stationary phase appears to act as a quasi-liquid layer, but as discussed below, it differs from a liquid in important ways. The separation of mixtures occurs as a mobile phase carries the analytes along the stationary phase. The retention of an analyte depends on its affinity for polar solvents, the nonpolar stationary phase, and other physical properties such as size and shape. Although the basic idea of the principles governing separation in an RPLC system appears simple, no comprehensive theory explains all the nuances of RPLC.

1.2 Theories of the Retention Mechanism

Several theories have been put forward to explain observed retention patterns and provide insight into retention under certain conditions. Most theories allow calculation of thermodynamic properties which can be compared with thermodynamic values obtained from actual separations. These thermodynamic values include the Gibbs free energy, equilibrium constants, entropy, and enthalpy. The more accurately a theory can describe and predict these thermodynamic properties, the more effective it can be used to model the retention process. Although the various theories account well for interactions under specific interaction conditions, no single theory accurately describes the retention behavior of all eluites under all conditions. This limits the ability for a theory to be used in modeling separations generally and reflects a deficiency in understanding of the retention process at the molecular level. Four major theories that attempt to explain molecular interactions of RPLC are the partitioning, solvophobic, adsorption, and slot models.

1.2.1 Adsorption Model

Adsorption is the simplest theory used to understand molecular interactions in RPLC separations. Here, retention is a result of adsorption to the surface. How well the analyte adsorbs to the surface depends on the chemical make-up of the molecule, primarily its polarity, and the chemical properties of the substrate. These chemical properties explain the retention mechanism of this theory. As the analytes are carried down the column by the mobile phase, they travel at different rates. The nonpolar analytes adsorb more strongly to the surface and remain on the column longer, whereas the polar analytes stay in the mobile phase and are carried off the column more quickly. If retention is governed by adsorption, the process can be described by

$$A^m + nS^a \leftrightarrows A^a + nS^m \quad (1.1)$$

where *n* denotes the number of displaced solvent molecules, *m* and *a* represent the mobile phase and adsorption layer, and A and S signify the analyte and solvent, respectively. However, the process shown in Equation 1.1 is only valid for a monolayer or bilayer of the adsorbed analyte in a uniform distribution. If this is not the case, that is if the analyte adsorbs in multiple layers and is minimally influenced by the adsorbed solvent, Equation 1.1 can be simplified to

$$A^m \leftrightarrows A^a \quad (1.2)$$

Monitoring the surface coverage as a function of concentration in a model system produces a surface isotherm. Thermodynamic values can be obtained from these isotherms and are discussed in more detail later in this chapter. From an isotherm, the equilibrium constant can be determined. This equilibrium constant describes the interactions of the analyte between the stationary and mobile phases.

1.2.2 Partitioning Model

Because adsorption occurs only on the surface of the stationary phase, the stationary phase has a limited number of active sites. This results in the surface of the stationary phase having significantly less potential for interaction than the bulk of the stationary phase; it has been generally assumed that adsorption has a smaller influence on RPLC retention than if the analyte partitions into the stationary phase.[2]

The partitioning theory assumes that the simplest way to model retention is to treat the stationary phase as an amorphous bulk fluid. This differs from the adsorption model, which assumes the stationary phase is not penetrated. In the partition model, separation occurs due to the competing affinity of the mobile and stationary phase for the solutes. Thus, as shown in

Figure 1.1, retention follows the oil/water partition coefficient of the analyte.[8] The retention mechanism in this theory is explained in three steps. First, a pocket is created in the stationary phase. Second, the analyte is transferred from a mobile phase pocket to the stationary phase pocket. And third, the mobile phase pocket is replaced by another solvent molecule. Figure 1.2 gives an example of a solute moving from the mobile phase (aqueous) to the model stationary phase (organic phase). Each step can be considered individually with molecular pair interactions, which are most favorable at a certain distance. Thus, as the analyte is carried down the column it can continually rearrange its position in relation to the stationary and mobile phases. As molecules rearrange, they constantly optimize the energy and entropy of the system as a whole. If the retention process of analyte A is due to partitioning, it is simply described by

$$A^m \leftrightarrows A^s \tag{1.3}$$

where m and s represent the mobile phase and the stationary phase, respectively.

Thermodynamic values from a partitioning system can be obtained by determining the amount of analyte that is partitioned into the nonpolar organic phase at different concentrations. This should produce an isotherm that is more complex than an adsorption isotherm. Although Equation 1.3 appears as simple as Equation 1.2, the practical application of Equation 1.3 is complicated by the depth of partitioning. The partitioning theory does not account for the stationary phase being bonded to the solid silica support. This bond can cause the stationary phase to experience a local structural rearrangement as analytes partition into it. The stationary phase is also generally cross linked, which can make the surface density of the stationary phase greater and makes deeper penetration of an analyte difficult than would be normally experienced from partitioning. However, correctly fitting a partitioning isotherm curve still yields an equilibrium constant.

Studies that attempt to understand retention using the partitioning theory generally use a polar solvent/nonpolar solvent system in order to extract partitioning data.[5] Carr et al.[9] used hexadecane to represent a carbon chain stationary phase and found the energies of the transfer of an alkylbenzene from a hydro-organic phase to the bulk hexadecane phase. Their results matched those observed in an RPLC separation. They concluded that the RPLC separation of small nonpolar analytes is primarily governed by partitioning.

1.2.3 Solvophobic Model

The two previously mentioned retention models use the stationary phase to account for separation. In contrast, the solvophobic theory attempts to explain retention of analytes on an RPLC column by relating retention to the mobile phase surface tension. This theory supposes that retention can be modeled in terms of the association of analytes with the solvent molecules. Retention in this theory is related directly to the interactions between the analyte and mobile phase. If the analyte has favorable interactions with the mobile phase, such as hydrogen bonding or other polar interactions, it remains in the mobile phase and is carried down the length of the column, and when the analyte does not experience these favorable interactions, it is forced out of the mobile phase.

Although in this model, the stationary phase plays a minimal role in retention, as shown in Figure 1.3, two configurations of the stationary phase are possible. If the analyte is nonpolar, it induces ordering of the carbon chains and the chains become extended in a fur-like configuration. However, if the analyte is polar then the stationary phase is predicted to collapse and stack onto itself in what is known as the stack configuration.[5] Despite the influence the analyte has on the stationary phase, the solvophobic theory assumes that retention is affected primarily by the mobile phase composition and not the by the length and surface density of the

nonpolar stationary phase.[2] However, Sentell et al.[10] varied the surface density of the stationary phase and found that retention ranges from no retention caused by the stationary phase to a maximum retention that followed bulk-phase partitioning. This is one example of how the solvophobic theory does not always agree with experimental data.

The solvophobic theory was the first theory to introduce the idea of measuring the free energy change of the interaction of an analyte with the stationary phase and the mobile phase. This information allows prediction of the retention of certain molecules.[5] Rafferty et al.[11,12] have shown that the mobile-phase contribution to the free energy of retention is unfavorable for all mobile-phase compositions studied, except for pure water. They also found that ΔG for the stationary phase is negative, as is the net free energy of retention, and its magnitude is slightly greater than ΔG of the mobile phase. Although this theory predicts some retention times, as shown above by Rafferty et al, it does not always produce the correct thermodynamics.

1.2.4 Slot Model

Most models explain retention in terms of the physical and chemical interactions of the analyte with the stationary phase and mobile phase, but the slot model uses the idea that cavities within the stationary phase retain molecules of a specific size and allow molecules of other sizes to pass. This theory has often been used to describe the retention of large aromatic compounds that are physically and chemically similar but are different in shape. Lippa et al.[13] studied these slots using alkyl chain dihedral analysis, a computer simulation technique that examines the dihedral angle of the stationary phase and determines the ordering of the chains. The authors found that for a C-18 stationary phase and a methanol mobile phase, the slots appear to be approximately 13 Å deep.

1.2.5 No Comprehensive Theory

These RPLC theories aid in the understanding of retention, yet no single theory explains every observation. Each theory provides insight into certain aspects of retention, but retention appears to be more than one simple idea. Even with all the research to date, it is still not possible to predict which molecular forces dominate in any given separation. Attempts to model separations have led to terms like "hydrophobic" and "solvophobic". These terms describe observed trends in the retention process. However, they do not always describe the trends correctly. Generally, nonpolar analytes show temperature dependence of retention, which is consistent with a hydrophobic interaction. However, some nonpolar analytes show no temperature dependence at all. Therefore, one cannot assume that all nonpolar molecules are driven primarily by hydrophobic interactions.[2]

Attempts at a comprehensive theory have involved combining these various ideas. In particular, in recent years the concepts of partitioning into the stationary phase and adsorbing to the surface have been united. If adsorption and partitioning principles contribute to the retention process, Equation 1.3 is no longer valid and should be combined with Equation 1.2 to produce

$$A^m \leftrightarrows A^a, \quad A^a \leftrightarrows A^s \tag{1.4}$$

where *s* refers to being partitioned into the stationary phase. Separation parameters, such as capacity factors, can then be calculated. The capacity factor, k′, is a measure of the distribution of the analyte between the stationary and mobile phase

$$k' = \mathrm{K}_{eq}\, {}^{V_s}/_{V_m} \tag{1.5}$$

where V_s is the volume of the stationary phase and V_m is the volume of the mobile phase. In a partition/adsorption-governed system, Nikitas et al.[14] showed that the capacity factor can be predicted by

$$k' = \lim_{n_A^m \to 0} \left(\frac{n_A^a + n_A^s}{n_A^m} \right) \tag{1.6}$$

where n_A^a, n_A^s, and n_A^m are the number of moles of the analyte adsorbed on the surface, partitioned into the stationary phase, and dissolved in the mobile phase, respectively This equation, and others like it, can predict capacity factors well, as seen in Figure 1.4. However, Figure 1.5 shows that when calculated results are fit to actual retention data, there is a large amount of error. Although the authors did not comment on the error, it appears to me that the deviations from the prediction show a systematic pattern that is dependent on the functionalization of the aromatic compound. This pattern of error is likely due to other factors of the retention mechanism that deal with size and shape effects that are not accounted for in these equations.

The primary disadvantage of such studies of capacity factors arises from how they are obtained. Capacity factors are measured from the time it takes analytes to elute from a column. Which in essence is only an average of what occurs over the duration of the time that the analyte is retained on the column. A more accurate way to model this would be to examine specific conditions at all points over the length of the column. This approach would provide a more accurate picture into what is actually occurring during retention.

1.3 Optimizing RPLC

Because separations do not always act the way theories predict, obtaining an ideal separation of a mixture is rarely achieved on a first try and instead the chromatographer must

make adjustments on the basis of educated trial and error. Furthermore, separations are affected by several operational factors, especially including conditioning of the column. Typically, prior to a separation, chromatographers flow a solvent or mixture of solvents through the column; this conditioning influences how molecules are retained on the column. Table 1.1 demonstrates how analytes eluted with the same solvent, in this case 100% acetonitrile, are retained for different lengths of time based on how the column was conditioned.

The effects of solvents with RPLC separations were further investigated by Le-Cong et al.[15] They investigated how changing the mobile phase influences retention. They conditioned an RPLC column with various solvents and then eluted the column with the same solvent it was conditioned with. Although it is not surprising to see different retention times with different solvents, interestingly, their results, as given in Table 1.2, showed a change in the elution order for the two solvents. For example, with ethanol, 6-nitrobenzene, the most polar of the four molecules, was eluted last from the column. However, with dichloromethane, 6-nitrobenzene became the second of the four analytes to elute from the column. The authors concluded that the phenomenon of elution reordering was caused by two factors. The first is a change in pressure required to maintain flow rate induced by the different viscosities of the solvents, and the second is the dipole moment of the solvent used for conditioning and eluting the column. Although this explanation may work in this case, it still does not assist in the optimization of all RPLC separations. This particular behavior of analytes with different solvents makes it difficult to predict retention times and elution order for any given separation.

1.4 Simulations

One way to better understand RPLC is to examine the interface of the stationary and mobile phase, which is where retention occurs. This can be accomplished in two ways. One can

use spectroscopic techniques to probe the stationary phase; these methods are discussed in more detail in Chapter 2. The other incorporates the use of computer simulations. Computer modeling has taken the understanding of retention to a new level. With computer modeling, a physical picture can be created to allow one to visualize the interactions occurring at the interface. It is an effective way to test RPLC theories because it creates a physical picture based on the set of parameters included in the simulation.

Lindsey et al.[11] showed that computer modeling confirms the fact that adsorption and partitioning both occur. Computer modeling has also shown that the mobile phase drastically influences the stationary phase. The mobile phase can affect the ordering and orientation of the carbon chains. It can also create different sized domains that affect the retention of analytes.[7] For example, this approach helps test the slot theory model.

Although computer simulations aid the understanding of retention, a computer simulation is only as good as the parameters it is programmed with. The flaw with the thermodynamic parameters currently used is that they are typically collected from data obtained at the end of the column, which can only reflect an average of what occurred over the length of the column. To more accurately model the specific environments experienced during the conditions on the column, information is needed all along the column. With accurate thermodynamic values, computer modeling will become even more powerful.

Table 1.1. Effect of Conditioning on Elution Rate[a]

Conditioning Step (% acetonitrile - % water)	100-0	80-20	50-50	20-80
naphthalene	6.50	7.12	10.50	11.75
6-nitrocrysene	7.30	9.27	10.90	12.77
chrysene	9.65	11.39	13.20	14.20
indeno(1,2,3-cd)pyrene	13.50	16.90	19.51	21.20

[a]Data from ref. 10. All elutions performed used a flow rate of 0.5 mL/min and 100% acetonitrile. Note how the amount of time the analytes remain on the column is influenced by the conditioning of the column.

Table 1.2. Comparison of retention times in minutes of analytes being eluted with different mobile phases[a]

Analytes	Ethanol	Dichloromethane
naphthalene	5.85	5.97
chrysene	6.00	6.20
indenopyrene	6.20	6.20
6-nitrochrysene	6.50	6.00

[a]Data from ref. 10.

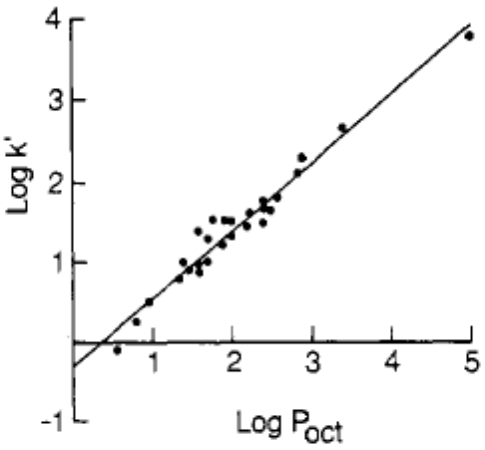

Figure 1.1. A comparison of the log of the capacity factor, k′, vs. the log of the oil/water partition coefficient of small analytes. Reproduced from ref. 8 with permission from the publisher.

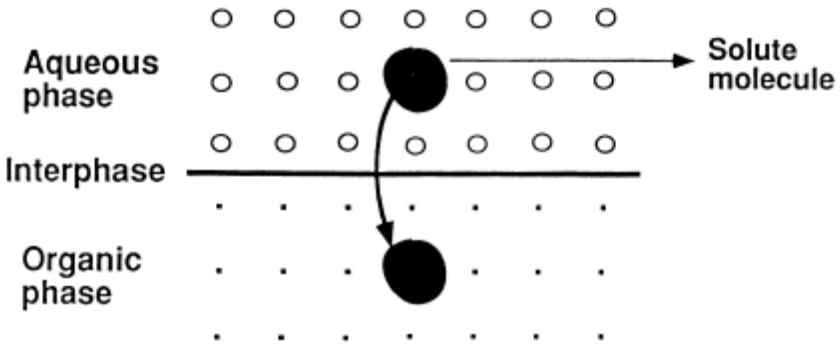

Figure 1.2. Depiction of a molecule partitioning between an aqueous phase and an organic phase. Reproduced from ref. 5 with permission from the publisher.

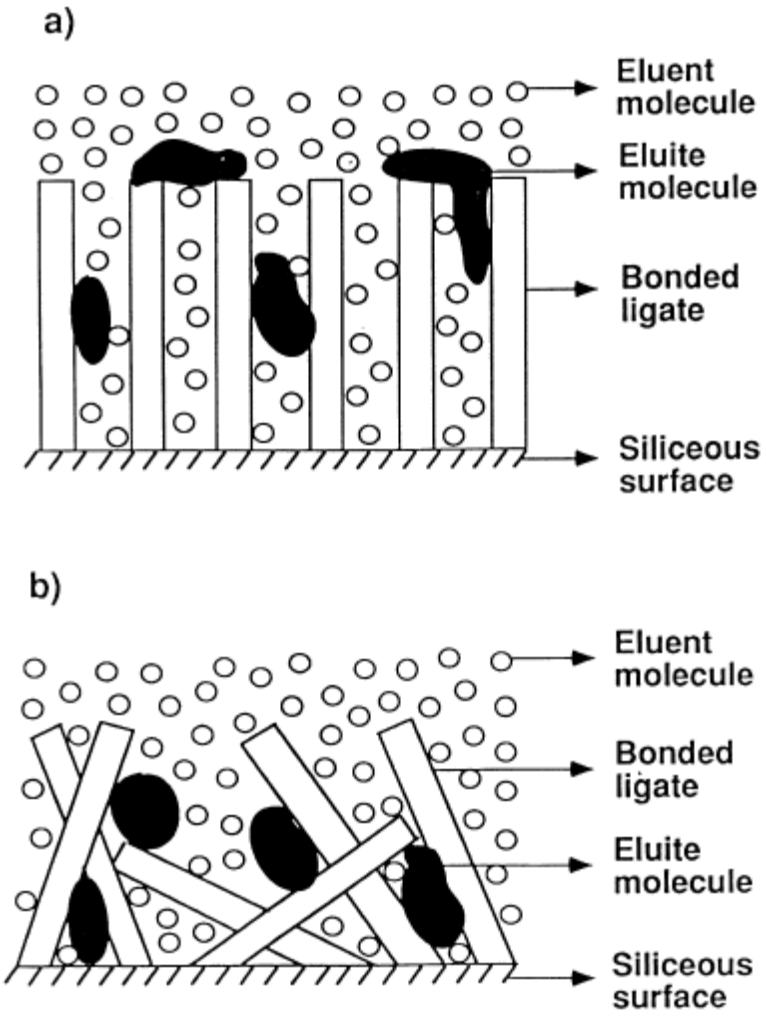

Figure 1.3. Illustration depicting the (a) "fur" and (b) "stack" configurations of the solvated stationary phase. Reproduced from ref. 5 with permission from the publisher.

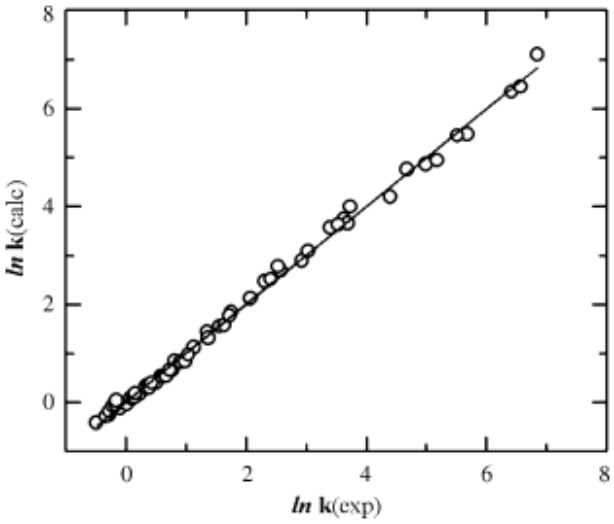

Figure 1.4. Plot of calculated ln k (referred to in this thesis as k′) vs. experimental ln k in isopropanol for various benzene derivatives. Reproduced from ref. 14 with permission from the publisher.

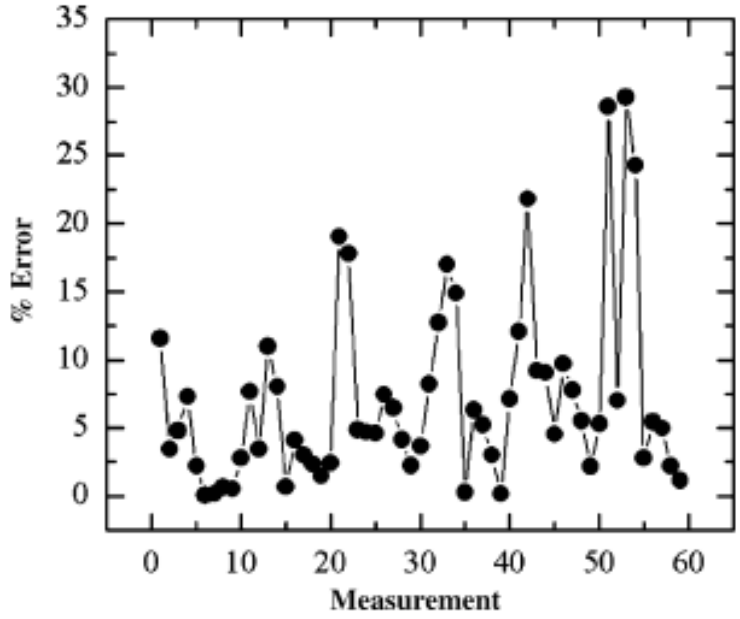

Figure 1.5. Percentage error between experimental and calculated retention times of various aromatic derivatives with an isopropanol mobile phase in a C-18 column. Reproduced from reference 14 with permission from the publisher.

Chapter 2

Spectroscopic Studies of RPLC

2.1 Investigation of RPLC using Raman, IR, and Fluorescence

Over the last few decades, several studies have incorporated the use of spectroscopic techniques, namely Raman, infrared, and fluorescence spectroscopy, to understand retention better.[16-24] These linear spectroscopic techniques have been used in an effort to understand retention by investigating changes that occur with the stationary phase and examining how retention is influenced by the mobile phase. These techniques can provide greater information than capacity factors alone because they can probe and obtain information along the length of the RPLC column.

M.W Ducey et al.[16,17] used Raman spectroscopy to investigate how stationary phases are influenced by temperature, surface coverage, and common mobile phase solvents. Their work simulated RPLC conditions to gain a deeper understanding of the principles that pertain to separations. Although their work was *ex-situ*, their results indicate that the conformational order and the alkyl chain interactions with other alkyl chains depends on both temperature and surface coverage. Their work also shows that nonpolar solvents are inserted into the alkyl chains, in essence opening up the stationary phase and allowing more interaction with the analytes. Polar solvents had the opposite effect; they influenced the stationary phase to become more ordered, creating fewer areas for analytes to interact with the stationary phase. These studies were achieved by examining the shifts in energy of the methylene peak in the Raman spectra.

The RPLC stationary phase has also been investigated with infrared spectroscopy. Srinivasan et at.[22] studied the surface coverage of C-18 modified silica gels using Fourier Transform Infrared spectroscopy (FTIR). They could detect how much of the silica gel surface

had been functionalized. This was achieved by monitoring the methyl wagging region in the infrared spectrum, normalized to the methyl deformation band. Their results show that as the surface density increases, the number of gauche defects lessens. In other words, the stationary phase appears more ordered.

Neumann-Singh et al.[23] also investigated RPLC stationary phases using FTIR. Their research analyzed conformationally sensitive vibrational modes. By monitoring these modes, they investigated conformational disorder of the stationary phase over a wide temperature range. They found that the conformational disorder is influenced by three things. First, as the temperature increases, the system becomes more disordered. Second, the proximity to parts of the silica surface influences disorder because the surface is not uniformly covered; therefore, some areas are unfunctionalized, and this leads to more freedom for nearby chains to move around. Third, the longer the attached carbon chain, the more freedom for movement there is at the end of the chain.

Although fluorescence is not an inherently surface specific technique, in recent years modifications have been made to fluorescence experimental setups which have allowed it to follow surface interactions. Harris et al.[24] used confocal fluorescence spectroscopy to track the movement of single molecules in an RPLC setup. They used octadecyl-rhodamine B molecules and imaged the fluorescence of these molecules as they moved within C18 functionalized silica particles. They could follow the movement of the octadecyl-rhodamine B and measure the amount of time the molecule remained involved with the stationary phase; they also found the intraparticle diffusion coefficient, which acted as a tool to resolve frame to frame behavior of molecules into moving and trapped parts. They concluded that these trapped events are evidence

of the heterogeneity of the interactions of the analyte with RPLC media and contribute to peak tailing in chromatographic separations.

Raman, IR, and fluorescence spectroscopy are very useful techniques from which much can be learned. Although Raman and FTIR techniques have tended to give results that confirmed expected properties, spectroscopic proof is useful to validate them. Unfortunately, these techniques have not revealed any new information that leads towards a greater understanding of what is specifically occurring with retention. Of the three techniques, fluorescence spectroscopy provides the most interesting and useful information because various polarization methods can be used to identify molecules trapped at the interfaces or to follow orientational diffusion. The main reason the other techniques fail to provide more insight is because the fundamental principles of these techniques do not allow differentiation of bulk molecules from surface molecules.

2.2 The Need for a Surface Specific Technique

Although the full mechanism of retention remains unknown, there is little debate that it occurs at the interface of the stationary and mobile phases. Raman and IR spectroscopy can provide insight into some aspects of RPLC, but they are not the best suited techniques to probe a surface specific event. The ideal method to investigate the retention process would utilize a technique that is surface specific and that can be used *in situ*. These requirements can both be met by using second-order nonlinear spectroscopy techniques, namely second harmonic generation (SHG) and sum frequency generation (SFG). In addition to fulfilling these requirements, they are also coherent processes, resulting in a directional signal. Because the work contained within this thesis focuses on SHG, SFG is not discussed in detail. But it should

be noted that SHG is the degenerate case of SFG, and the selection rules for both techniques are identical.

Spectroscopic techniques can be described in terms of the electric susceptibility of a material, χ. The induced polarization of the material depends on its susceptibility and the strength of the electric field, E, with higher-order components of the susceptibility becoming more important as the field strength increases:

$$P(t) \propto \chi^{(1)}E_1 + \chi^{(2)}E_1E_2 + \chi^{(3)}E_1E_2E_3 + \ldots \quad (2.1)$$

The first term in equation 2.1 leads to linear spectroscopy techniques, such as Raman and IR. Linear techniques require a single input beam. The second term in equation 2.1 results in second-order nonlinear spectroscopic techniques such as SHG. These second-order techniques require two input beams, although they can be collinear. The third and higher terms in Equation 2.1 give rise to higher-order optical techniques, which require addition input beams and are not discussed here.

The intensity of the SHG signal, I_{SHG}, is directly proportional to the two input electric fields $E_{\omega 1}$ and $E_{\omega 2}$ at frequencies ω_1 and ω_2, according to[25]

$$I_{SHG} \propto \left|\chi^{(2)}\right|^2 E_{\omega 1}E_{\omega 2} \quad (2.2)$$

As shown in Equation 2.2, the SHG signal depends directly on the intensities of the two input light pulses. Because SHG uses identical input beams, the SHG signal is directly proportional to the square of the two input fields.

2.3 SHG: A Coherent Surface Probe

SHG requires coherent input beams. As these coherent beams interact at an interface, they produce a third coherent signal beam. Producing a coherent, and directional, signal beam gives SHG a clear advantage over linear spectroscopic techniques, which generally scatter signal in all directions. Another advantage of SHG is that it can be used probe molecules ordered at an interface;[26] this advantage is discussed in greater detail later in this chapter. Because three beams are involved, SHG is considered a three-wave process. The frequency of the signal is the sum of the two input frequencies. In Figure 2.1 it can be seen that signal is produced as the two input photons combine together through an electronic state, incorporating the use of a virtual state. It is most accurate to view this as a concerted transition, rather than happening sequentially.

Because SHG is a coherent process both energy and momentum are conserved. Energy is conserved as the two frequencies of light interact at the surface to produce SHG signal. This is mathematically described by

$$\omega_1 + \omega_2 = \omega_{SHG} \tag{2.3}$$

Where, in the case of SHG, $\omega_1 = \omega_2$. Because momentum is also conserved, the angle at which the signal is produced can be predetermined by

$$\omega_1 cos\theta_1 + \omega_2 cos\theta_2 = \omega_{SHG} cos\theta_{SHG} \tag{2.4}$$

where θ_1 and θ_2 are the angles of incidence of ω_1 and ω_2, respectively, and θ_{SHG} is the angle of ω_{SHG}. Equation 2.4 can be rearranged to easily find θ_{SHG}:

$$\theta_{SHG} = \frac{cos^{-1}(\omega_1 cos\theta_1 + \omega_2 cos\theta_2)}{\omega_{SHG}} \tag{2.5}$$

This angle is the direction that the SHG signal leaves the surface. In the collinear case, when both photons come from the same laser pulse, the SHG signal angle is identical to the reflected input beam signal. And the advantage of being spatially offset is lost.

2.4 The Second-Order Nonlinear Susceptibility, $\chi^{(2)}$

Whereas most of the advantages of SHG arise from the conservation of energy and momentum, the greatest advantage of SHG comes from signal production only from interfaces. This advantage arises as a result of the phase matching conditions of $\chi^{(2)}$, a 3rd rank tensor. The nonlinear susceptibility, $\chi^{(2)}$, of any medium is shown in Figure 2.2 and can be described in three dimensional space with a 27-element tensor.[26] If the medium described by $\chi^{(2)}$ is isotropic, meaning it is completely random with no preferred direction, then all 27 elements of $\chi^{(2)}$ are exactly zero. When all the elements are zero then no SHG signal is produced. Media that are isotropic exist in the bulk portion of a solution.

In anisotropic environments, such as a surface, not all of the tensor elements are zero. Determining which elements are zero and which are not zero can be found by analyzing an arbitrary surface. This is easily accomplished by assigning Cartesian coordinates to the surface with z-axis being defined as the axis normal to the surface and the x-axis and y-axis are on the surface. As operations are performed on this arbitrary surface, such as rotations or mirroring, if the surface looks identical the tensor value can only be a zero. For example, if we take the surface and rotate it 180° about the z-axis, see Figure 2.3a, (x) becomes (-x) and (y) becomes (-y), but (z) remains (z). Analyzing this rotation with the $\chi^{(2)}_{(xyx)}$ tensor element, it can be easily seen that that only way for it to be equal to the $\chi^{(2)}_{(-x)(-y)(-x)}$ is if $\chi^{(2)}_{(xyx)} = \chi^{(2)}_{(-x)(-y)(-x)} = -\chi^{(2)}_{(xyx)} = 0$. When inspecting the rest of the tensor elements, it is found that whenever there is an odd number

of x's or y's in the tensor element that tensor element must be zero. This reduces the total number of possible non-zero tensor elements from 27 to 13.

The number of independent non-zero elements can be further reduced if a 90° rotation is applied around the z-axis, see Figure 2.3b. This does not force any elements to be zero, but it does reduce the number of independent elements. This rotation leads to the following six relationships of the remaining tensor elements:

$\chi^{(2)}_{(zxy)} = \chi^{(2)}_{(zyx)}$, $\chi^{(2)}_{(zxx)} = \chi^{(2)}_{(zyy)}$, $\chi^{(2)}_{(xzx)} = \chi^{(2)}_{(yzy)}$, $\chi^{(2)}_{(xxz)} = \chi^{(2)}_{(yyz)}$, $\chi^{(2)}_{(xzy)} = \chi^{(2)}_{(yxz)}$, and $\chi^{(2)}_{(xyz)} = \chi^{(2)}_{(yxz)}$.

Including $\chi^{(2)}_{(zzz)}$ gives only seven independent non-zero terms. This value can be reduced one final time by applying a mirror plane through the z-axis, see Figure 2.3c. This mirror plane transforms an (x,y) vector into a (y,x). Applying this final operation leads to four remaining non-zero terms remain that are completely independent:

$\chi^{(2)}_{(zzz)}$, $\chi^{(2)}_{(xzx)} = \chi^{(2)}_{(yzy)}$, $\chi^{(2)}_{(xxz)} = \chi^{(2)}_{(yyz)}$, and $\chi^{(2)}_{(zxx)} = \chi^{(2)}_{(zyy)}$

These four non-zero tensor elements shed light on the different ways that an interface can be probed. Plane polarized light that contains the z-axis is called p-polarized, or parallel, light. If the light is perpendicular to the z-axis, containing any combination of the x-axis and y-axis, it is called s-polarized, or perpendicular. These polarizations can be used to describe the four independent tensor elements: *ppp*, *sps*, *ssp*, and *pss*. These conventional listings describe the three beams involved in the SHG process starting with the polarization of the highest energy photon, the SHG signal, and descending to the polarization of the lowest energy photon.

2.5 Past studies with VR-SFG

In recent years, several researchers have begun to understand how useful SFG can be to increase the understanding of retention. These studies have incorporated the use of vibrationally resonant SFG (VR-SFG) and have primarily examined the stationary phase. Much can be learned from the graduate work of Brent Horn,[27] Robert Baker,[28] and Arthur Quast[29] of Brigham Young University. The thesis work of Arthur Quast investigated a model RPLC stationary phase using VR-SFG and found that the stationary phase is influenced by even small amounts of pressure; however, his work showed the solvent does not appear to influence the stationary phase as much as was expected. Marie Messmer's group at Lehigh University used SFG to do extensive research on stationary phase structure at ambient pressures and found that conformational changes of the stationary phase on the surface of fused silica occur in three stages.[30-34] Recently, Sly et al.[35] demonstrated how nonlinear spectroscopic techniques can be used to determine surface binding kinetics and thermodynamics of test drugs as they adsorbed and desorbed from a model lipid bilayer. They used a variant of SHG to determine adsorption and desorption rates as well as the equilibrium constant.

Although it is unnecessary to provide an extensive review of the work performed by these people, it is important to note some of the findings of previous work. The thesis work of Art Quast concluded that the stationary phase does not undergo substantial structural changes when it is exposed to elevated pressures. His work, as well as Brent Horn's and Robert Baker's work, were the stepping stones to the idea of probing analytes interacting with the stationary phase using a second order non-linear technique.

The work contained within this thesis focuses solely on probing adsorption of a test analyte to a model stationary phase. It is intended to build on the research that has already been

performed on model RPLC systems using VR-SFG. Although the VR-SFG experiments provide insight into the stationary phase, the setup is limited in its ability to probe the analytes. The SHG experiments provide the necessary means to probe the electronic state of the analytes and can help create an understanding of how the analytes interact on the surface of the stationary phase. Each experiment provides deeper insight into a part of the mechanism of retention, and combining the findings from both methods will give a much more complete picture of retention. This deeper understanding of RPLC separations will come by incorporating the results from analyzing the structure of the model RPLC stationary phase using VR-SFG with the surface interactions of test analytes to the stationary phase determined with SHG under identical conditions.

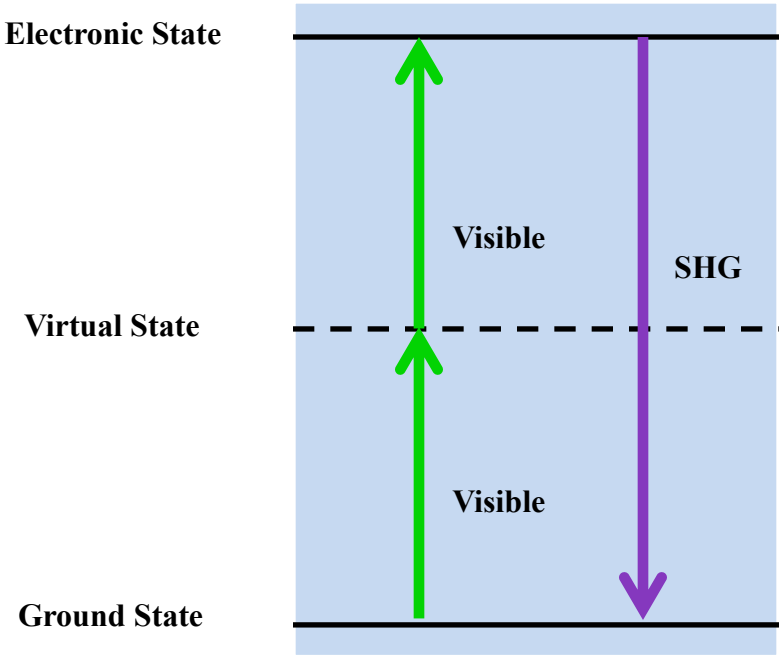

Figure 2.1. Energy level diagram of SHG. SHG signal is produced simultaneously as a two visible photon perturbs the molecule up to an electronic state. The SHG signal is coherent and directional.

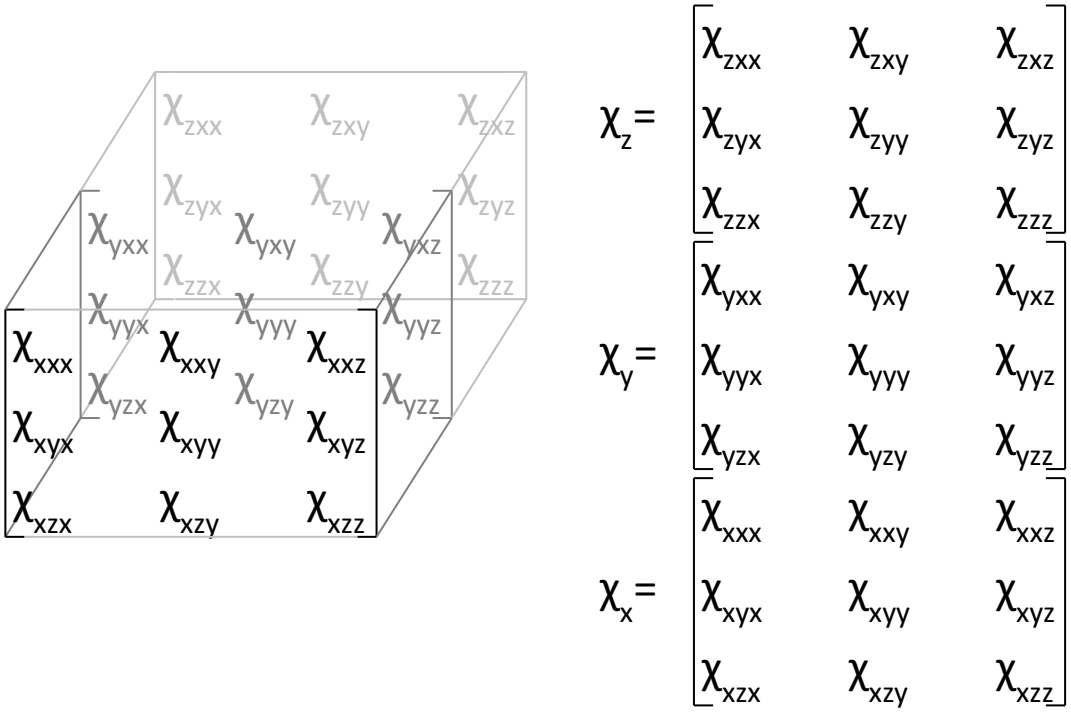

Figure 2.2. The second order nonlinear susceptibility, $\chi^{(2)}$, depicted to visually illustrate all 27 tensor elements. $\chi^{(2)}$ is a 3rd rank tensor that describes nonlinear susceptibility in 3-dimensional space.

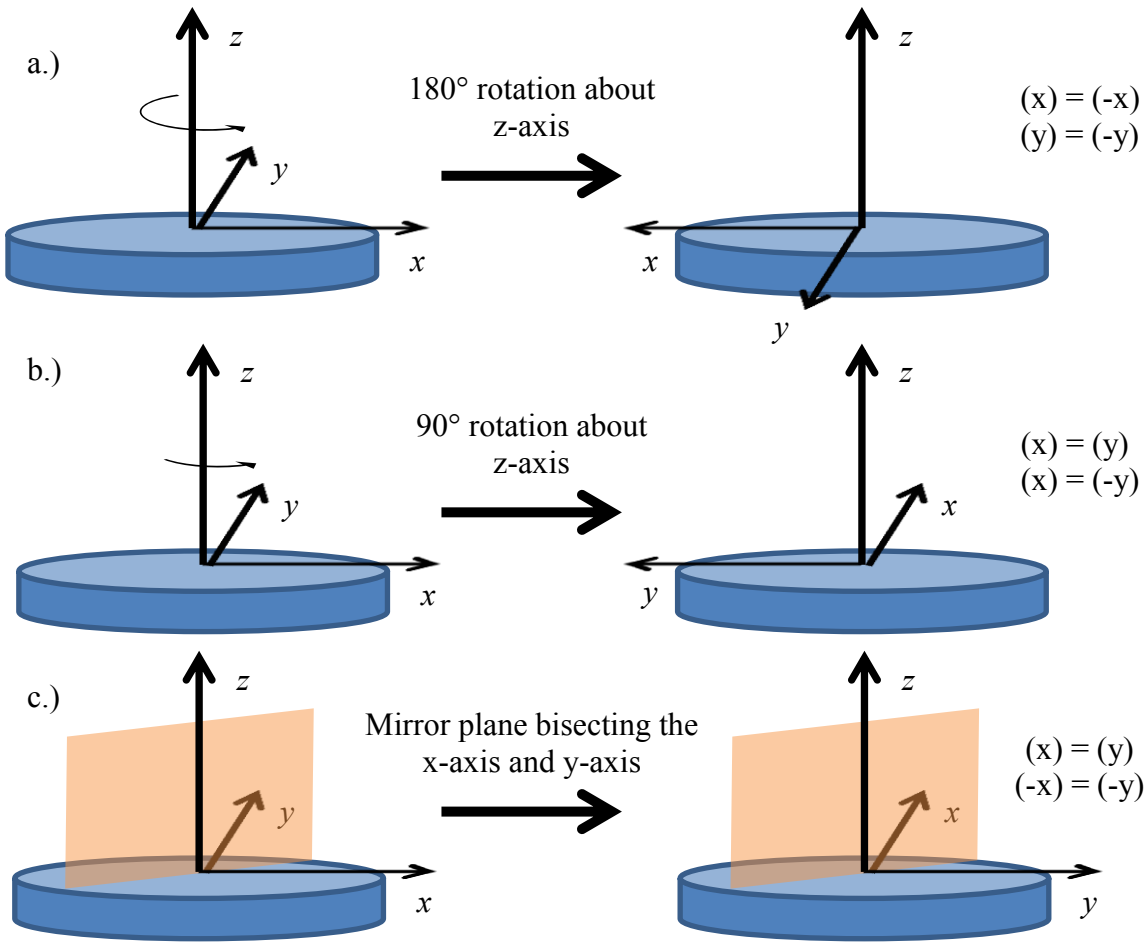

Figure 2.3. A series of depictions demonstrating how different operations applied to an azimuthally symmetric surface can be used to determine what tensor elements must be zero and which ones are independent of others. (a) applies a 180° rotation operation about the z-axis axis; (b) applies a 90° rotation operation about the z-axis, and (c) does a mirror plane operation that includes the z-axis in the mirror plane.

Chapter 3

Investigating Adsorption to Model C18 Stationary Phase With SHG

3.1 Introduction

Reversed-phase liquid chromatography (RPLC) is one of the most widely used tools for analytical separations.[2] As simple as an RPLC system seems to be, over the years many theories have been adapted in attempts to more accurately depict what is occurring with retention; however, today there is still no comprehensive theory of RPLC.

Attempts at more fully understanding the retention process have led to probing RPLC columns with a variety of spectroscopic techniques, such as Raman, IR, and fluorescence spectroscopy. Although these techniques give insight into separations, they are generally incapable of giving a complete picture. The problem with such linear spectroscopic techniques arises because the techniques detect everything, the bulk concentration in addition to whatever is adsorbed to the surface. However, retention occurs at the stationary phase. To obtain an accurate picture of what is occurring at during retention, a surface specific technique is required.

Sum-frequency generation (SFG) and second harmonic generation (SHG) are second order nonlinear spectroscopic techniques that are inherently surface specific. This surface specificity is because of the non-linear susceptibility, $\chi^{(2)}$, of the medium. If the medium described by $\chi^{(2)}$ has a point of inversion, then all 27 tensor elements of $\chi^{(2)}$ are exactly zero and no signal is produced. Non-zero tensor elements exist only when the medium is azimuthally symmetric. This type of medium exists at interfaces, such as surfaces. For this reason, SHG can be used to probe analytes as they adsorb to a C18 surface. This work uses SHG for the first time on a model RPLC system to produce surface isotherms.

The primary purpose of the work contained within this thesis is to understand in greater detail what is occurring at the interface between the stationary phase and analyte. This is accomplished by using SHG to probe a model stationary phase. To probe the interface, a test group of analytes was chosen. This group consists of the six polyaromatic hydrocarbons (PAHs) that are composed of four aromatic rings. These compounds were chosen because they have similar physical and chemical properties but are retained differently on an RPLC column. Table 3.1 shows the different retention times of these analytes as they are eluted with methanol. The difference in retention can be assumed to be primarily caused by the differing shapes of the molecules. Although the entirety of the project will include looking at the other PAHs in the test group, the first analyte of the test group to be investigated is pyrene. All of the work contained within this thesis focuses on investigating pyrene on a model stationary phase.

3.2 Physically Modeling RPLC

RPLC columns are typically packed with functionalized silica gel beads ranging from 2.5µm to 5µm. However, probing the surfaces of these particles is difficult using nonlinear spectroscopic techniques. This difficulty is due to the spherical nature of the particles which causes the SHG signal to mostly cancel itself out. Instead of struggling to isolate a small amount of SHG signal, common practice has been to use a physical model that represents the nonpolar stationary phase. This is achieved by functionalizing a fused silica surface with octadecyltrichlorosilane (OTS). The fused silica surface acts as a model because it consists of surface silanols that react with the OTS reagent. The reaction is

$$C_{18}H_{37}SiCl_2 - Cl + Si - OH_{(surface)} \rightarrow HCl + C_{18}H_{37}SiCl_2 - O - Si_{(surface)} \qquad (3.1)$$

The procedure for performing surface functionalization is discussed later in this chapter. Planar functionalized silica produces larger signals than functionalized spheres.

Previous work applying *in-situ* conditions with VR-SFG used a functionalized 1-inch diameter fused silica disc and collected the retroreflected signal. While the retroreflected VR-SFG signal is sufficient for studies regarding the stationary phase, not enough signal is produced using this method for SHG analysis. Greater SHG signal can be collected from a total internal reflection setup. However, it is impossible to obtain total internal reflection using a fused silica disc, Figure 3.1a. Instead, total internal reflection for the SHG experiment is achieved by using a fused silica prism, Figure 3.1b.

3.3 Experimental

3.3.1 Laser and Optics

The SHG experiment is based on Nd:YAG laser (Coherent Infinity Laser) that produces upwards of 250-300 mJ of 1064 nm light per pulse. The 1064 nm light is doubled to 532 nm light. The doubling crystal is then tuned or detuned so that each pulse consists of between 60-100 mJ. The beam has a diameter of ~8mm and a pulse duration of 6ns. Before the beam reaches the surface, it is attenuated with a half-wave plate and a beam splitting cube down to between 20-22 mJ per pulse before being shrunk down to ~2 mm in diameter.

As mentioned in chapter 2, different polarizations of light can be used to probe the independent tensor elements; however, with these experiments it was advantageous to probe all the elements at once. This is achieved by rotating the beam splitting cube to a 45° angle. The attenuation is still controlled by adjusting the angle of rotation on the half-wave plate. This angle allows the light to be broken into two components, an s-polarized portion and a p-polarized

portion. As these polarizations interact at the surface, all non-zero tensor elements can be probed at once. This setup is preferred because the experiment is probing analytes adsorbed on the surface and the orientation of the analytes is not important for the current study. Also, probing all elements produces the greatest amount of signal.

SHG signal is produced as the 532 nm light is directed to the back of a fused silica prism, which is functionalized with a C-18 chain. As the analytes adsorb to the surface, 266 nm light is produced as the 532 nm photons interact with the molecules at the interface. If the analytes have a real electronic state at 266 nm, the amount of SHG signal is enhanced. Figure 3.2 shows the UV-Vis absorption of pyrene. Because pyrene absorbs at 266 nm, there is an electronic state that exists and the pyrene signal is greater significantly greater than if it could not absorb 266 nm light. The SHG signal is directed to two filters and a monochromator, which are used to filter out any scattered 532 nm light. The signal is detected and amplified with a photo-multiplier tube (PMT), and 100 laser shots are averaged using a boxcar averager. The processed signal is collected on a computer using a DAX port. A diagram of the experimental setup can be seen in Figure 3.3.

3.3.2 Functionalizing Fused Silica Prisms

Custom UV-grade fused silica prisms were obtained from Almaz optics. The prisms have a 67° angle on both sides and have a 1-inch square back and are ½ inch tall, see Figure 3.2. Before the prisms are functionalized, they are put in a 50 mL beaker contacting roughly 30 mL of a *piranha* solution (3:1 sulfuric acid to 30% hydrogen peroxide) for 2 hours. (Caution: Piranha is a strong oxidizer and is very corrosive, extreme care and proper equipment must be used when handling.) This cleaning is required to ensure that the surface is free from particulate contamination. The *piranha* solution is then poured out and the prism is rinsed with purified

water (18 MΩ resistance) until the water is neutral. The prisms are then rinsed with acetone, dichloromethane, chloroform, and again with dichloromethane. (Note: All organic solvents are HPLC grade.) Each solvent is used until there are no more traces of the previous solvent. The prism is then placed in a 50 mL beaker of dichloromethane and placed in a glove box. The glove box is purged and filled with nitrogen 10 times to remove any reactive oxygen and water from the environment. Following the final purge, a 1 mL sample of OTS is added to the reaction beaker and the beaker is sealed with duracil and parafilm. After the OTS reagent is added, the reaction shown in Equation 3.1 begins. The reaction is allowed to proceed for at least 24 hours. When the prism is removed it is rinsed again with copious amounts of dichloromethane, acetone, water, acetone, dichloromethane, and finally chloroform. It is then sonicated in chloroform for 10-15 minutes. Following this, the prism is rinsed with methanol and is sonicated in methanol for 20 minutes followed by a second rinsing with methanol and 20 more minutes of sonicating in methanol. Contact angles were taken on the prism using a goniometer to determine the effectiveness of the functionalization. Functionalized prisms are then stored in methanol.

3.3.3 Sample Mount

The sample mount used for the SHG experiments was specially cut from a block of Teflon by the Precision Machine Lab at Brigham Young University. The block was cut to have a square 1-inch insert where the prism can settle in. On the inside of the insert was a special cut for an o-ring. In the middle of the o-ring cut are two drilled holes that extend through the block. These holes serve as the inlet and outlet when flowing fluid through the sample mount. The bottom of the mount is bolted to a magnetic base which allows it to be reproducibly placed in the path of the laser for the SHG experiment. The face of the sample mount has four threaded holes for posts to be inserted which are used to secure the prism in place.

Before a prism is attached to the sample mount, it is important to ensure that the sample mount is clean. Successfully cleaning the sample mount is done by unscrewing the support post and placing it upside down in 200 mL of a *piranha* solution. Turning the mount upside down prevents that magnetic base from being exposed too much to the *piranha*. The sample mount is allowed to sit in the piranha solution for at least 12 hours. The sample mount is rinsed with purified water (18 MΩ) until the water coming off of the mount is neutral. Following the water rinse it is rinsed with acetone, dichloromethane, chloroform, and methanol. After it has been sufficiently rinsed with methanol, the input and output of the mount are blocked. The sample mount is then laid so it is face up and a neoprene o-ring is placed on it. Methanol is added until it bulges just over the o-ring. Now the prism is removed from its methanol solution and placed on top of the o-ring. The prism is then tightened down using Teflon braces and wing nuts. The prism should be on the sample mount as tightly as possible. (Note: Before the prism is attached it has been sonicated twice in methanol, each time for at least 20 minutes.) To ensure a clean prism, the surface is rinsed with chloroform followed by methanol which is then blown dry with nitrogen gas.

3.3.4 Making Pyrene Solutions

Pyrene solutions are prepared using 100 mL volumetric flasks. Before using the flasks, they are rinsed with acetone, dichloromethane, chloroform, and methanol. The rinsing process went up through these solvents, back down then and repeated to forward process once more. Enough pyrene is then weighed out to form a 1 mM concentration and is added to a volumetric flask and topped off with methanol. The 1 mM solution is sonicated to ensure the pyrene is fully dissolved. This concentration is diluted down to 0.1 mM by pipetting 10 mL and adding it to an empty volumetric flask which is then also topped off with methanol. Dilutions continue in like

manner until concentrations as low as 0.0001 mM are obtained. Other concentrations are made by pipetting 10 mL of a higher concentration multiple times. Solutions are sonicated before they are used to flush the sample mount.

3.3.5 Peristaltic Pump

Initial SHG experiments used a glass syringe to flush 4-5 mL of the concentration through the sample mount. This flushing was most effective when starting with pure methanol and every flush using a slightly higher concentration than was previously in the sample mount. This method required between three and four hours for the system to reach equilibrium whenever a flushing occurred. Unfortunately, how quickly the mount was flushed and the amount of time the system was given to equilibrate greatly influenced the amount of signal that would be produced. This was circumvented by incorporating a peristaltic pump.

Peristaltic pump tubing is attached to the inlet port at the back of the sample mount and has the other end placed in a beaker of methanol. The tubing is then attached to the pump. Polypropylene tubing is then attached to the outlet port at the back of the sample mount and is placed in a waste beaker. The peristaltic pump is set to pump ~0.4 mL per minute. Several mL of methanol is run through the sample mount to ensure that the functionalized surface of the fused silica prism is completely clean. Solutions are pumped through the sample mount continuously whether or not a scan is occurring. When it is time to move onto the next concentration, the inlet tubing is removed from the current concentration and rinsed with methanol and placed in a beaker containing the next concentration to be studied. The pump also solves the problem of not knowing the bulk concentration of the analyte, which I discuss later in this chapter.

3.3.6 Obtaining Isotherms

Adsorption isotherms describe the equilibrium of molecules at an interface at constant temperature. They directly represent the number of molecules that are bound at the surface as a function of the bulk concentration in the solution. The most frequently used isotherms are the linear isotherm, Freundlich isotherm, the Langmuir isotherm, and the BET model. Out of these isotherm models, the simplest one is the Langmuir isotherm.

The Langmuir isotherm depends on of four basic assumptions. First, the surface is homogenous. Second, all adsorption sites are equal. Third, each site can hold only one molecule. And fourth, there is no interaction between adsorbed molecules with molecules attempting to adsorb in an adjacent spot. Isotherms that follow a Langmuir pattern can be fit to SHG data with

$$I_{SHG} = \left(\frac{K_{eq}}{1+K_{eq}}\right)^2 \tag{3.2}$$

Once the prism is securely attached to the sample mount and the sample has been sufficiently flushed with methanol, collecting a surface isotherm of pyrene can begin. Isotherms are obtained by increasing the concentration of pyrene by controlled intervals and monitoring the resulting signal. Initial isotherms went to concentrations as high as 10 mM, see Figure 3.5a.

Because methanol can order up at the interface, it too produces SHG signal, but once a complete set of concentrations has been collected, the methanol signal can be assumed constant and subtracted out from all signals. The isotherm is then normalized by dividing all the signals by the signal obtained from the 0.01 mM solution. Normalizing the signal is required because of day-to-day variations of the max SHG signal. Adjustments in alignment and placement of the

prism on the sample mount allow for slight differences. When properly normalized, these differences are nullified.

3.4 Results/Discussion

Preliminary data using the glass syringe to flush the system is shown in Figure 3.5a. Although this method produces a surface isotherm, I found that error is introduced into the experiment because the glass syringe inhibits the ability to ensure identically reproducible flushes. Because of this error, the curve does not fit a Langmuir isotherm model well. Nevertheless, upon examining the lower concentrations and the signal produced from them, an additional isotherm curve is apparent at lower concentrations, which is shown in Figure 3.5b. This discovery led me to focus primarily on the lower concentration isotherm. Initial attempts at reducing noise included longer equilibration times and slower flushes. The reasoning for this came as I monitored the time profile of the signal; an example is shown in Figure 3.6. As I flushed the system quickly, I noted how a spike occurred in the signal, and over time the signal dropped. I came to believe that this spike was due to a larger than normal concentration of analyte forced onto the surface from the quick flush. Over time, it would equilibrate with the rest of the system and the signal would decrease.

As I changed the experimental setup to include a three hour equilibration time the results became more reproducible. Upon combining two days of data collection, a cleaner isotherm was obtained, which is shown in Figure 3.7. This isotherm can be fit well using a Langmuir model. From this fit, an equilibrium constant of 1.7×10^4 is obtained. However, the inherit problem with this result is that the actual concentration of the bulk solution is unknown because of the depletion of analyte in the solution as it adsorbs to the surface.

This problem was overcome with the addition of the peristaltic pump. As the pump continuously moves solution through the sample mount, the analytes in the bulk equilibrate with the stationary phase. This continues until equilibrium is reached and the bulk concentration in the sample cell matches the bulk concentration used to flush the system. This modification gives a better idea of what the equilibration time is; a time profile of the signal is shown in Figure 3.8. Using the pump caused the signal to no longer decrease over time. Because the bulk concentration is higher using the peristaltic pump, it can be assumed that the surface coverage is also higher. Figure 3.9 shows an isotherm obtained with the peristaltic pump. This curve is a more accurate representation of the actual equilibrium between the stationary phase and the mobile phase. The curve in Figure 3.9 was fit to a Langmuir isotherm model, and it can be seen that a Langmuir model fits the curve well. From this fit, an equilibrium constant of 7.5×10^4 is obtained with a 95% confidence interval of $\pm 1.9 \times 10^4$. Although the fit has an SSE of 0.0008 and an R^2 value of 0.9989, the large standard deviation arises from the nature of the fit. To minimize the standard deviation, additional points must be taken at the lower concentrations where the curve is more prominent. This pronounced effect of obtaining an equilibrium constant 4.4 times larger emphasizes the importance of knowing the bulk concentration of the solution. Although the signal does not change for any given actual concentration, if the bulk concentration is not initially in equilibrium with the stationary phase then it decreases as the analytes adsorb to the surface. If this decrease was correctly accounted for, the isotherm curves could be normalized and would match.

The equilibrium constant can be related to the capacity factor by:

$$K_{eq} = k'\beta \tag{3.3}$$

where *Keq* is the equilibrium constant obtained from the isotherm, k' is the capacity factor of pyrene for retention in a system with a phase ratio β, the ratio of the volume of the mobile phase to the volume of the stationary phase.

The equilibrium constant is also directly related to the Gibbs free energy change of the system:

$$\Delta G^{\circ} = -RTln\ K_{eq} \tag{3.4}$$

where *R* is the gas constant and *T* is the temperature in kelvin. The Gibbs free energy of the interaction between the stationary phase and analytes is a key parameter for the various theories and for computer simulations. Because this is the actual free energy for the analyte adsorption, computer models could provide a better idea of how the analyte interacts with the stationary phase. It is important to note that at this stage of our investigation, experiments have been done only at ambient pressure, so the results apply only to the conditions observed at the end of an RPLC column. As the study moves forward, it will be important to extend the measurements to higher pressures and ultimately to mixed phases. I discuss more about what the next steps in our investigation need to be in Chapter 4.

3.5 Conclusions

At low concentrations a Langmuir isotherm model fits the data well. This means that at lower concentrations the interaction between the analytes and the stationary phase can be described with Langmuir principles. This can be explained by both surface adsorption and partitioning. While Langmuir isotherms are generally used to describe adsorption, some partitioning models also produce Langmuir isotherms. However, it is possible that both methods occur simultaneously and still produce a Langmuir isotherm.

A key finding of my work is to illustrate the importance of knowing the true concentration of the bulk solution in equilibrium with the stationary phase. This significantly affects the curve of the isotherm, and the K_{eq} extracted from the curve. Comparing the K_{eq} from Figure 3.7 to the K_{eq} obtained from Figure 3.9 shows this. The equilibrium constant obtained from knowing the bulk solution in the equilibrated system was 4.4 times greater than when the bulk concentration was not known.

After accurately determining the equilibrium constant from the surface isotherm, K_{eq} can be used to find $\Delta G°$ of the system. This is the first step in obtaining all the thermodynamic values that can then be used to improve computer calculations. Obtaining the other thermodynamic values can be acquired by adjusting the temperature of the solution; I discuss this further in Chapter 4.

Knowing the thermodynamics of analyte adsorption increases the understanding of how retention is influenced by thermodynamics. However, understanding the equilibration rates is also important for the future of this research. A significant finding of this research is that the equilibration time of this experimental setup is on the order of tens of minutes. This is important especially in light of the fact that chromatographic bands pass over any part of the column on the order of seconds. However, it is important to note that this experimental setup does not account for the closeness of the stationary phase on neighboring silica gel beads. This close proximity is likely to decrease the total equilibration time, but must be further studied. A more complete picture of retention of analytes at the RPLC interface will be understood as thermodynamic values are combined with kinetics of the interactions of the analytes with the stationary phase.

In addition to thermodynamic information dealing with retention, a fuller understanding will not be obtained until the thermodynamic values can be combined with kinetic values. The kinetic values can be obtained when monitoring the rates of adsorption and desorption, this is discussed more in Chapter 4.

Table 3.1. The retention of the six PAHs that contain 4 aromatic rings.[a]

Analyte	Retention Time[b]
Pyrene	4.06
Triphenylene	4.19
benzo[c]phenanthrene	4.20
benz[a]anthracene	4.43
Crysene	4.46
Naphthacene	5.04

[a]Data collected from http://chrom.tutms.tut.ac.jp/JINNO/DATABASE/
[b]100% MeOH and flow rate of 1.0 mL/min

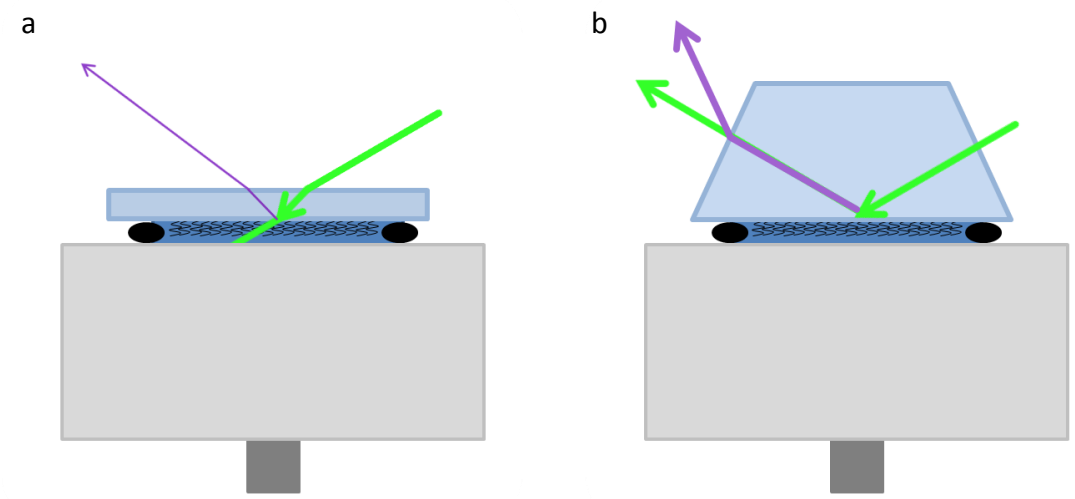

Figure 3.1. (a.) shows SHG performed on a window and (b.) shows SHG perfomed with a prism. The prism serves two purposes. First, it allows for greater signal to be collected due to total internal reflection of the photons. Second, when the signal beam exits the prism it is refracted differently than the reflected signal beam. This allows the beam to be spatially filtered.

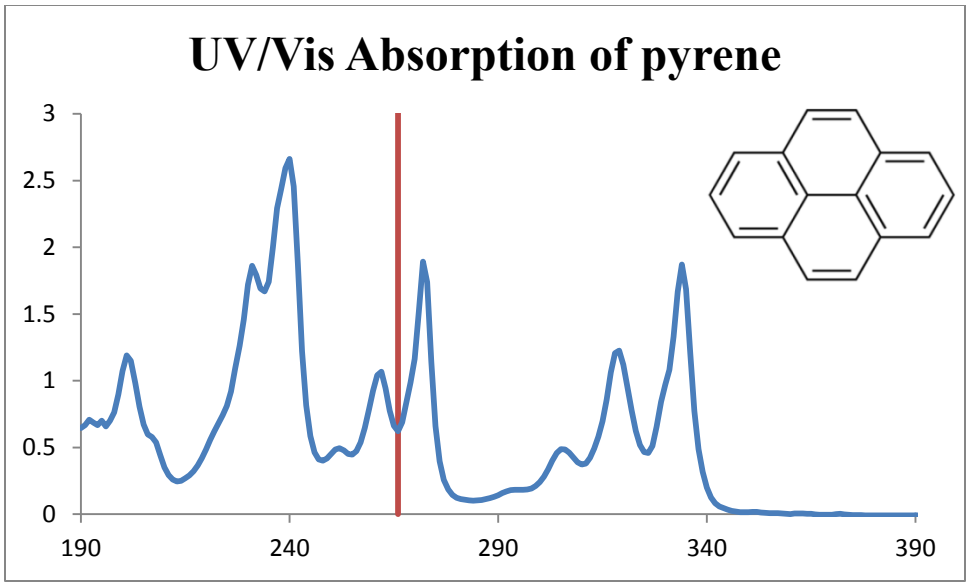

Figure 3.2. The UV-Vis absorption of pyrene. The red line indicates 266 nm.

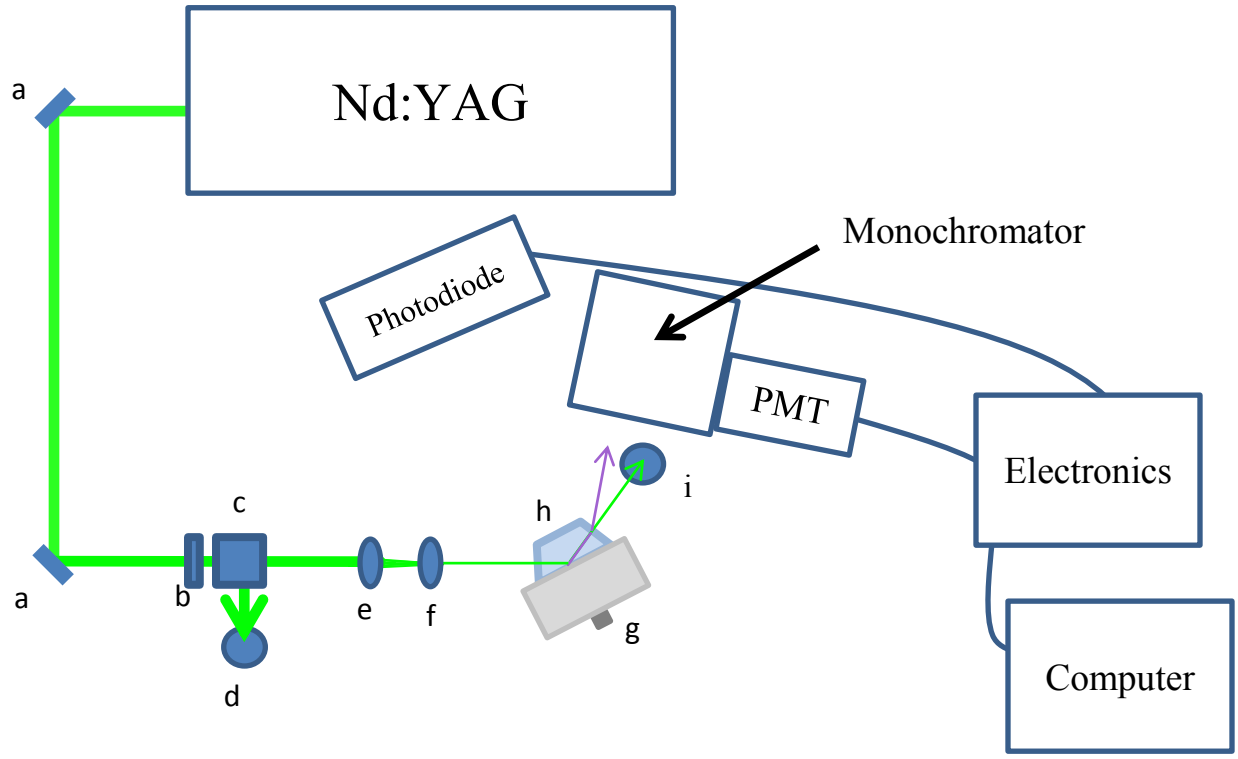

Figure 3.3. The SHG setup used to probe the model stationary phase. (a) dichroic beam steering mirrors. (b) half-wave plate to rotate the light to a 45° angle. (c) beam splitting cube, that when combined with (b) works as a beam attenuator. (d) opper beam dump. (e) and (f) recollimating lenses. (g) sample cell. (h) the prism that has been functionalized. (i) glass horn beam dump.

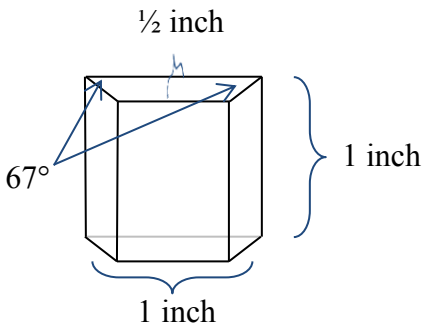

Figure 3.4. Diagram explaining dimensions on Almaz Optics custom fused silica prism.

a.)

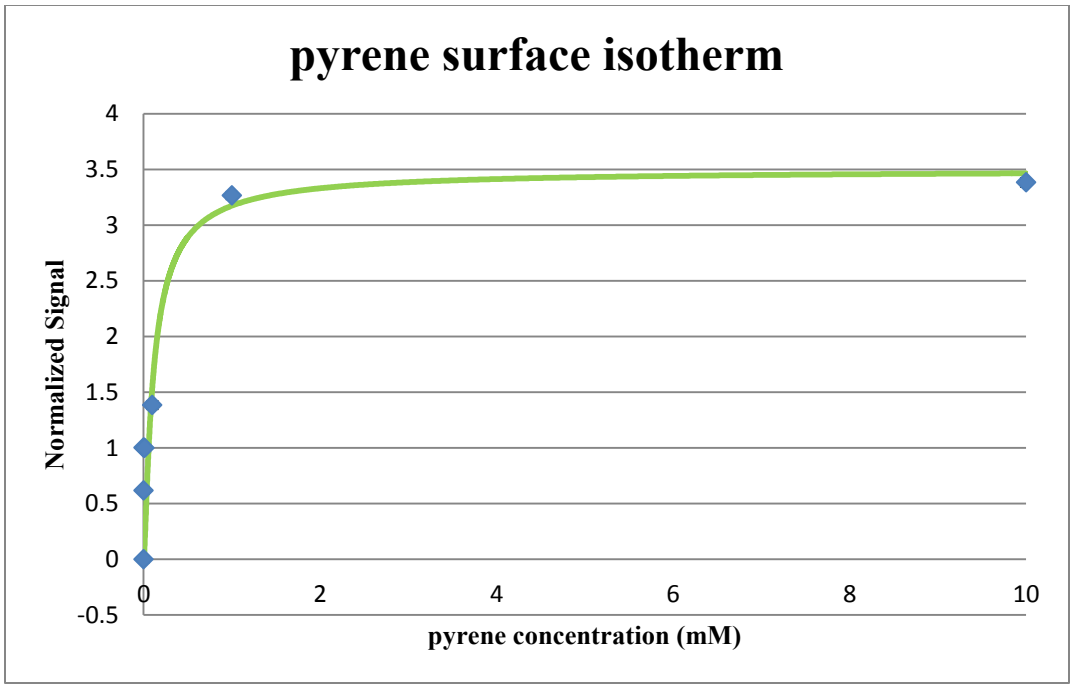

b.)

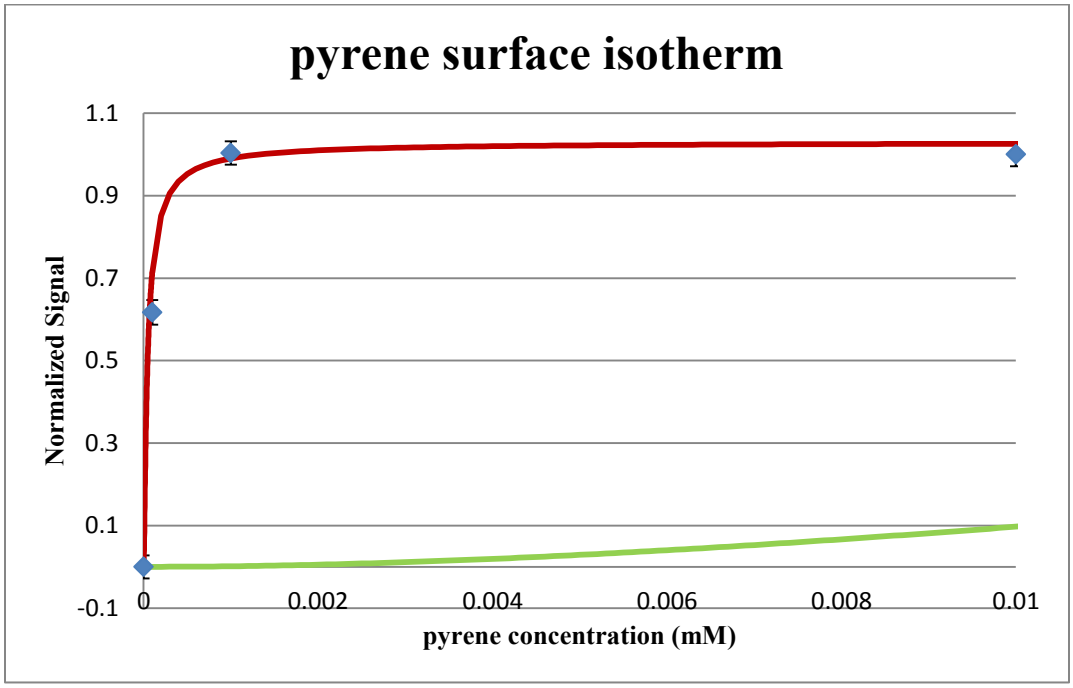

Figure 3.5. (a) shows the higher concentration isotherm fit to a Langmuir model. (b) shows the lower concentration isotherm, where the red line is a Langmuir fit and the green is the extrapolated line of the Langmuir fit from part (a.) for the higher concentration curve. The apparent discrepancy is likely due to poor flushing procedures that have since been altered.

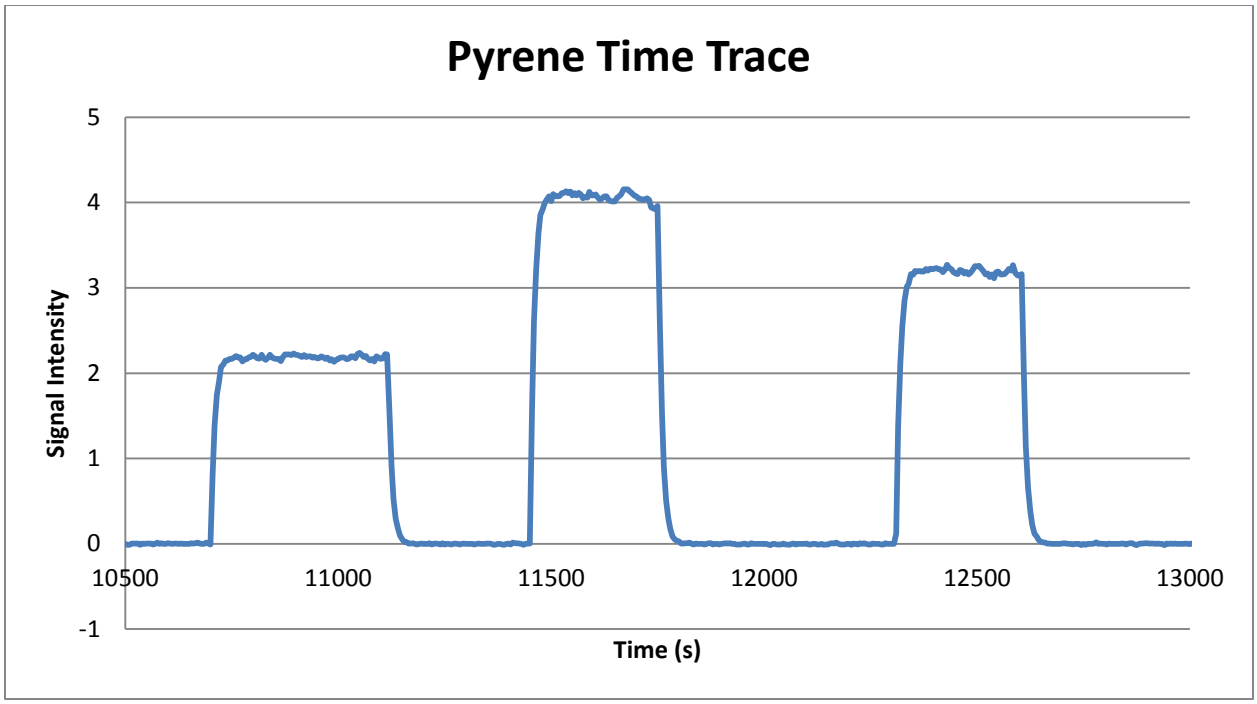

Figure 3.6. A time trace of the SHG signal when using the glass syringe method. The left peak is the methanol signal that has equilibrated. The middle peak was collected right after the system was flushed with 0.0001 mM pyrene using the glass syringe method. The right peak is 15 minutes after the system was flushed. Note how the pyrene signal decreased over time.

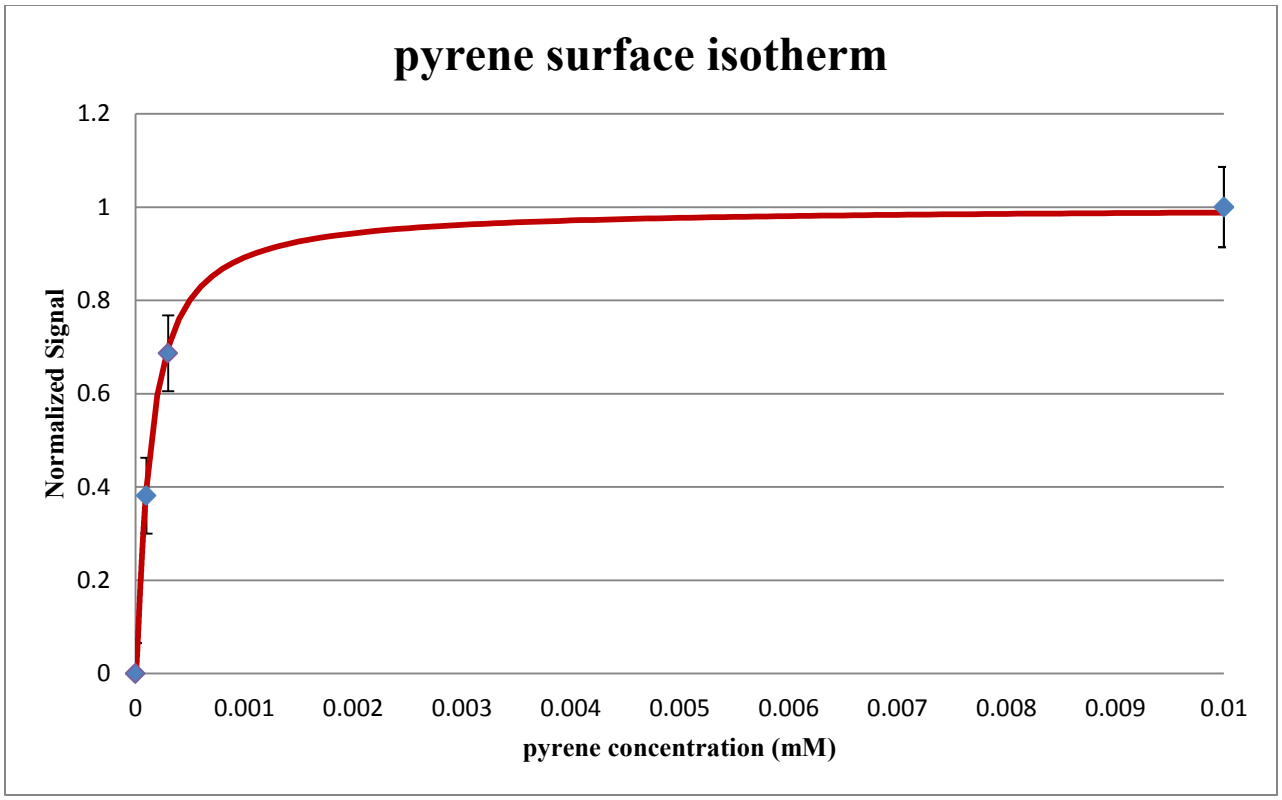

Figure 3.7. Pyrene isotherm obtained after equilibrating for more than three hours per concentration. This curve is fit with a Langmuir isotherm model.

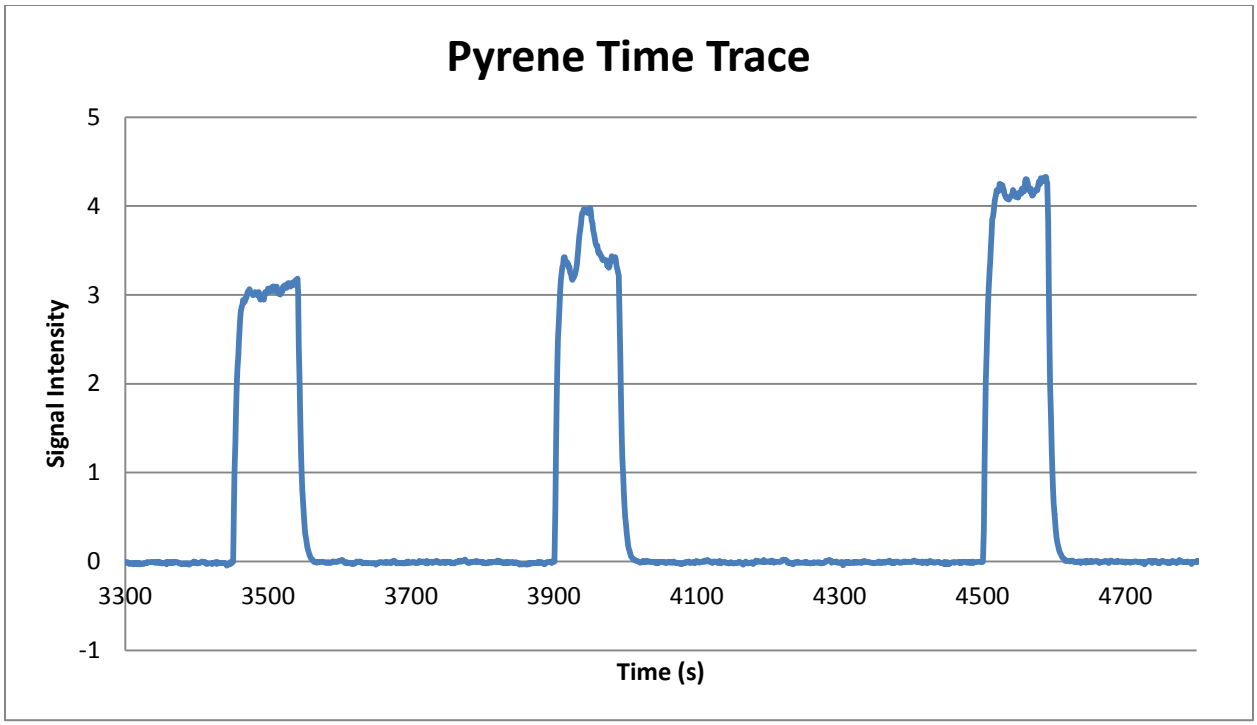

Figure 3.8. A time trace of the SHG signal with the peristaltic pump for flushing the system. The left peak was the stabilized methanol signal. The middle peak represents 5 minutes after the pump was changed to 0.0001 mM pyrene. The right peak represents the 0.0001 mM signal 15 minutes after the flush. Note the rise in signal over time.

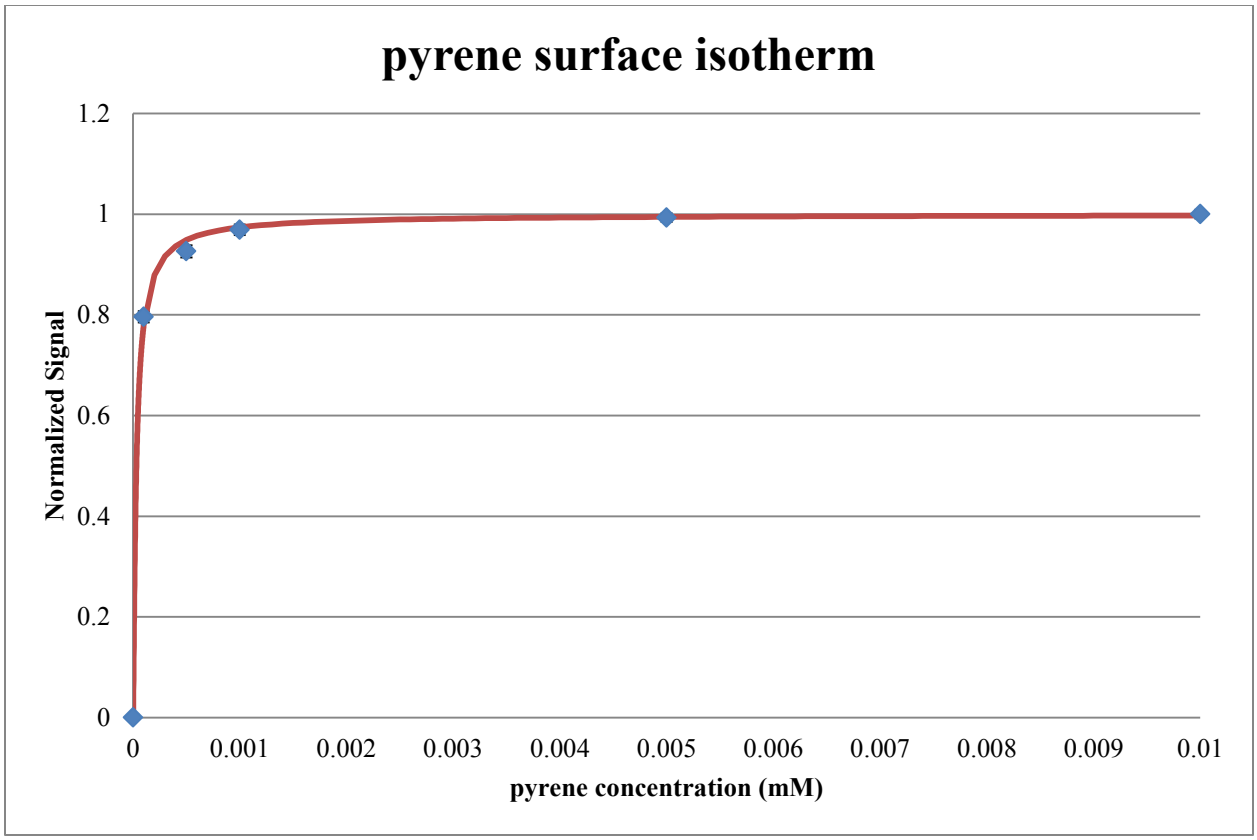

Figure 3.9. Isotherm obtained with the peristaltic pump modification. The curve is fit with a Langmuir isotherm model.

Chapter 4

Future Work

4.1 ΔH° and ΔS°

Obtaining the other thermodynamic values, ΔH° and ΔS°, will be achieved by performing experimental runs at different temperatures. To do this, the solution must be slightly heated as well as the sample mount. The temperature must be carefully measured to accurately give the temperature of the solution within the sample mount. Each isotherm must be obtained at a constant temperature and from the change in the equilibrium constant value, ΔH° can be determined using the Van't Hoff equation:

$$\partial \ln k/\partial T = \Delta H°/RT^2 \tag{4.1}$$

Once ΔG° and ΔH° are known, ΔS° can easily be calculated from the definition of Gibbs free energy,

$$\Delta G° = \Delta H° - T\Delta S° \tag{4.2}$$

After knowing all the thermodynamic values for ambient pressure, the next step will be to pressurize the system and obtain ΔG, ΔH, and ΔS at higher pressures. Thermodynamic values gained from within modeled RPLC column conditions will lead to greater insight into the thermodynamics of separation. These parameters can be incorporated into computer simulations and would the ability of computer modeling to accurately depict what is occurring during retention at specific RPLC column conditions.

In addition to varying the pressures, the experiment is also dependent on obtaining isotherms under similar conditions using other analytes of interest, namely the remaining PAHs that contain 4 aromatic rings and other analytes of similar size and shape. Greater insight will be

obtained by understanding how the size and shape of an analyte influences all of the thermodynamic properties of the separation. Also, the thermodynamic values of the different analytes can be used to more effectively relate the retention times to the shape of the analytes.

4.2 Understanding RPLC Separations

To understand the driving forces of RPLC and create a universal theory that can predict retention, the work performed within this thesis must be combined with additional information. The setup within this research provides insight into the thermodynamics of the interaction of analytes with the stationary phase. This provides a greater understanding of many driving forces of RPLC, but a complete story will be had by understanding how the stationary phase interacts with the analyte, which can be done using VR-SFG, and by understanding how quickly the process occurs, which can be done by studying the kinetics of adsorption.

4.2.1 Combining VR-SFG and SHG

Whereas obtaining thermodynamic data relating to the analyte will provide greater insight than is currently had, it is only part of fully understanding RPLC separations. More can be learned by understanding how the stationary phase reacts to the presence of analytes under certain conditions. This will be achieved by continuing the studies using SHG to examine the analytes and by including VR-SFG experiments that will examine the same conditions but will probe the orientational and conformational structure of the stationary phase. Understanding how the stationary phase interacts with the analyte and mobile phase is just as important as understanding how the analyte interacts with the mobile and stationary phase. As these two methods are combined, a model can be created that would be able to explain the observations that are specific to the interface of the RPLC stationary phase.

4.2.2 Kinetic Studies of RPLC

Studying the kinetics of the adsorption process can be achieved by monitoring the SHG signal against time. To do this, it will be imperative to use a faster laser rep rate to overcome the noise that would be present for faster studies. The system will need to equilibrate first with methanol and then switch the inlet of the peristaltic pump to flow the concentration of the analyte of interest. Performing this experiment with the six test PAHs should produce interesting results. Because the shape of the PAHs is similar, it is quite possible that the thermodynamic values are not very different. However, because of the different shapes, I would think that the analytes without a permanent dipole, like pyrene, would be able to equilibrate more quickly.

4.3 Recycling the Prisms

Recycling the custom fused silica prisms will be important as a practical matter for future experiments. This can be done by applying MasterPolish 2 Polishing Medium (Buehler, P/N 40-6376-032) to an 8-inch microcloth PSA (Buehler, P/N 40-7218). After being polished, the prism can be exposed to UV light for at least 5 minutes. Following this, the prism can be submerged in *piranha* solution followed by being re-functionalized. These recommendations are based on suggestions given by Krystal Sly of the Conboy group from the University of Utah. Initial refunctionalizing experiments should be attempted on fused silica windows, which are considerably cheaper, and should be characterized with the VR-SFG setup to ensure that the functionalized coating is fully removed. The main purpose of attempting to recycle the custom fused silica is for financial reasons.

4.4 Final Thoughts

I feel that I have been able to get a lot accomplished with this experiment; unfortunately most of my advances have occurred in the last year. During my first year I struggled to obtain

any form of signal. I am pleased to have the system up and working with the problems I am aware of fixed. I believe that this experiment has a lot of potential and there is still much that can be done. I feel proud knowing that I setup something from which a lot of research can be performed.

Appendix

A1 Trouble Shooting Experimental Problems

This section is intended for the benefit of future researchers who will be working with this experiment or on others similar to it. It is my hope that they will learn from my pitfalls and will have even more success. When I started my master's degree in 2011, my project was envisioned to use an ultraviolet-visible SFG technique. This required the use of two photons, one in the UV and one in the visible range, that interact in a counter propagating fashion. For alignment purposes, both photons were 532 nm. This initial setup was performed more in an SHG fashion. However, it differs from the current setup because the photons came from two distinct laser beams. One beam came directly from the Nd:YAG laser and the other was 532 nm light from the OPO system that was pumped from a 355 nm breakoff of the Nd:YAG laser. As I attempted to align the beams correctly to produce SHG signal, the PMT picked up a lot of scattered light, and I could never detect if I had any signal. The large amounts of scattered light led me to attempt using a monochromator to isolate out the 266 nm signal. Despite great effort, I never found signal at 266 nm. Eventually, I decided to characterize the wavelength of the OPO, and found that the wavelength was roughly 1 percent off from what the computer stated was the wavelength. For example, if the computer read 500 nm, it was roughly 5 nm off and actually showed up closer to 495 nm. Unfortunately, correcting for this did not result in obtaining SHG signal.

Eventually, I considered the idea of abandoning the UV-Vis technique for an SHG approach. This was still done in a similar counter propagating fashion, but instead of having two different laser beams, a single laser beam was directed to the prism surface and then reflected with a dichroic mirror back to the same spot on the surface. While this technique initially

seemed more promising, I was still never able to detect SHG signal. Because I still had no luck with this method, I decided that I would simplify the experiment even further. This was done by removing the dichroic mirror that reflected the beam back to the prism. With the beam hitting the surface in one direction, the experiment was now set up in co-propagating fashion.

The idea of total internal reflection has been a part of this experiment from the start. However, the way it was obtained has changed over the course of the experiment. Initial attempts with the UV-Vis system used a cylindrical lens, but this approach never was able to work properly. Eventually the lens was switched to a right angle prism that had the top ground off and then polished. Even though this allowed total internal reflection, it still never worked to produce SHG signal. Eventually I ordered custom prisms that were angled at 67°, which matched the total internal reflection angle of fused silica. These prisms made alignment easier because the reflection off the prism surface was along the beam path when the prism was properly aligned. Incorporating these custom prisms with the co-propagating SHG method produced signal.

Even though I had found signal, I was using an oscilloscope and averaging scans on it. After I had saved them onto a flash drive, then I had to integrate the area of the peak myself. This led to a long and tedious effort to try to collect the data. Upon the suggestion of Dr. Farnsworth, I added a boxcar averager/gated integrator. This allowed be to select what area to collect data within as well as how many shots to average. This drastically reduced the amount of time required to collect and analyze data. And another great benefit of the boxcar averager was the ability of connecting the data collection directly to the computer.

Now that I had successfully found signal and could directly collect data on the computer, I still struggled with the stability of the laser power. The Nd:YAG laser that I was using had significant fluctuations in power, which caused fluctuations in the signal and much noise in the data. I initially attempted to remedy this by adding a photodiode to the system to monitor the fluctuations. While this method to correct for power fluctuations worked, the fluctuations were cause for other problems, including hot spots in the beam profile. These hot spots damaged some of the optics and led me to find another laser that would work as well or better. Fortunately, there was a laser in the adjacent lab that, in Dr. Asplund's words, is better for my experiment in every way. This new laser had better power control, had an adjustable repetition rate, and had a better beam profile. Adjusting to the new laser took a little time, and I found out that it takes about 2–3 hours before it is fully stabilized, but after those few hours of warming up, this new laser performed exponentially better than the previous one.

Even with a change in laser, I still noticed some interesting things as I took long scans. Little things like bumping the table affected the signal. Eventually, I determined that the PMT was the culprit of these problems. If the PMT was even slightly bumped or moved, the signal was drastically affected. When I changed to a different PMT, the signal became very stable and even bumping the counter did not influence the signal. The reason switching the PMT was so effective was likely because the new PMT could be fit directly onto the monochromator and had a larger active area.

One final problem that I had to overcome with the experiment was the flushing process. Every time I flushed the system I always got a rise in the signal. This would occur even if I was flushing methanol when the sample cell which was already equilibrated with methanol. This led to long hours of making sure that the system was fully equilibrated before I could start collecting

data. However, I finally decided that creating a flow cell would be a more effective way to flush the system. I was able to do this by borrowing a peristaltic pump from Dr. Farnsworth. After the pump was added to the experimental setup, I attempted to see how well it worked with flushes. To do this, I put the peristaltic pump inlet into a new beaker of methanol and continued to take scans as it constantly was flushing the sample mount with this new methanol solution. The results showed that the system never spiked upon the addition of methanol. In fact the signal stayed identically the same. The addition of the peristaltic pump allowed for the system to be equilibrated at a greater rate due to the consistent and slow pumping.

A2 What I Have Learned That Makes the Experiment Work Better

There are several things that I have learned that make this SHG experiment work even better. A lot of the things that I have learned have been incorporated into the experimental setup and can be read about in A1, but I learned other things that are not part of the physical setup of the experiment but are still useful.

Because the experiments still take some amount time to equilibrate, the repetition rate of the laser is not that important. And I have found that it is actually better to have the laser at a 10 Hz repetition rate for the sake of the lifetime of the flash lamps. Increasing the repetition rate would allow quicker data collection, but there would be a significantly greater amount of wasted flashes during the down time. A faster repetition rate would be useful for kinetic studies, otherwise, a lower repetition rate works well.

For inspection of the profile of the beam, the most important part is to make sure there are no hot spots. However, if there are places where the beam is not as bright as the rest, this is okay as long as it is consistent. Another important aspect of the beam is to ensure that the beam

is truly collimated before it enters the prisms. This can be tested easily enough by examining the size of the reflected beam from the surface of the prism.

It is also a very good idea to ensure that the outside of the prism is clean; this can easily be done by rinsing the prism with a little chloroform and then methanol and drying it off with nitrogen. If the surface is not clean, you risk the chance of the laser damaging the surface. It also can produce more scatter that may not be as consistent over time.

Another check I have learned is very easy, but can save a lot of headaches is checking the signal to make sure it really is signal and not just 532nm scatter. Do this by blocking the monochromator with a glass slide and see if the signal disappears. If the signal does not completely disappear, it means that there is green scatter. Check to see if you can determine the source of the green scatter. I have the system setup so when SHG experiments are performed, there should never be any green signal that reaches the PMT. Also, it is very important to make sure you are collecting both the PMT signal and the photodiode signal and not just collecting one of them twice. This can be done while checking for signal. Make sure on the LabView program one of the signals disappears and another doesn't disappear. Although this seems like a very simple check, it can save a lot of time.

The final thing that I have learned is to avoid duracil and parafilm during the course of data analyses. The main problem arises because we are using such small amounts of analyte that if plasticizers were to leach from the duracil or parafilm, it could influence the signal. It seems to be fine to use these for the long storage, or overnight storage, of items but should be avoided when actually collecting isotherms.

References

(1) Horvath, C.; Melander, W. *Journal of Chromatographic Science* **1977**, *15*, 393.

(2) Dorsey, J. G.; Dill, K. A. *Chemical Reviews* **1989**, *89*, 331.

(3) Rafferty, J. L.; Siepmann, J. I.; Schure, M. R. *Journal of Chromatography A* **2012**, *1223*, 24.

(4) Rafferty, J. L.; Siepmann, J. I.; Schure, M. R. *Journal of Chromatography A* **2009**, *1216*, 2320.

(5) Vailaya, A.; Horvath, C. *Journal of Chromatography A* **1998**, *829*, 1.

(6) Zhang, L.; Rafferty, J. L.; Siepmann, J. I.; Chen, B.; Schure, M. R. *Journal of Chromatography A* **2006**, *1126*, 219.

(7) Wick, C. D.; Siepmann, J. I.; Schure, M. R. *Analytical Chemistry* **2004**, *76*, 2886.

(8) Butte, W.; Fooken, C.; Klussmann, R.; Schuller, D. *Journal of Chromatography* **1981**, *214*, 59.

(9) Carr, P. W.; Li, J. J.; Dallas, A. J.; Eikens, D. I.; Tan, L. C. *Journal of Chromatography A* **1993**, *656*, 113.

(10) SENTELL, K.; DORSEY, J. *Analytical Chemistry* **1989**, *61*, 930.

(11) Lindsey, R. K.; Rafferty, J. L.; Eggimann, B. L.; Siepmann, J. I.; Schure, M. R. *Journal of Chromatography A* **2013**, *1287*, 60.

(12) Rafferty, J. L.; Sun, L.; Siepmann, J. I.; Schure, M. R. *Fluid Phase Equilibria* **2010**, *290*, 25.

(13) Lippa, K.; Sander, L.; Mountain, R. *Analytical Chemistry* **2005**, *77*, 7862.

(14) Nikitas, P.; Pappa-Louisi, A. *Journal of Chromatography A* **2009**, *1216*, 1737.

(15) Andrade-Eiroa, A.; Le-Cong, T.; Nguyen, M.-L.; Dagaut, P. *CheM* **2011**, *1*, 62.

(16) Ducey, M. W.; Orendorff, C. J.; Pemberton, J. E.; Sander, L. C. *Analytical Chemistry* **2002**, *74*, 5576.

(17) Ducey, M. W.; Orendorff, C. J.; Pemberton, J. E.; Sander, L. C. *Analytical Chemistry* **2002**, *74*, 5585.

(18) Doyle, C. A.; Vickers, T. J.; Mann, C. K.; Dorsey, J. G. *Journal of Chromatography A* **1997**, *779*, 91.

(19) Doyle, C. A.; Vickers, T. J.; Mann, C. K.; Dorsey, J. G. *Journal of Chromatography A* **2000**, *877*, 25.

(20) Doyle, C. A.; Vickers, T. J.; Mann, C. K.; Dorsey, J. G. *Journal of Chromatography A* **2000**, *877*, 41.

(21) Liao, Z.; Orendorff, C. J.; Pemberton, J. E. *Chromatographia* **2006**, *64*, 139.

(22) Srinivasan, G.; Sander, L. C.; Muller, K. *Analytical and Bioanalytical Chemistry* **2006**, *384*, 514.

(23) Neumann-Singh, S.; Villanueva-Garibay, J.; Muller, K. *Journal of Physical Chemistry B* **2004**, *108*, 1906.

(24) Cooper, J. T.; Peterson, E. M.; Harris, J. M. *Analytical Chemistry* **2013**, *85*, 9363.

(25) Conboy, J. C.; Kriech, M. A. *Analytica Chimica Acta* **2003**, *496*, 143.

(26) Bain, C. D. *Journal of the Chemical Society-Faraday Transactions* **1995**, *91*, 1281.

(27) Horn, B. A., Disseratation, Brigham Young University, Provo, UT, 2001.

(28) Baker, L. R., Thesis, Brigham Young University, Provo, UT, 2007.

(29) Quast, A. D., Thesis, Brigham Young University, Provo, UT, 2011.

(30) Liu, Y.; Wolf, L. K.; Messmer, M. C. *Langmuir* **2001**, *17*, 4329.

(31) Liu, Y.; Wolf, L. K.; Messmer, M. C. *Abstracts of Papers of the American Chemical Society* **2001**, *221*, U378.

(32) Henry, M. C.; Wolf, L. K.; Messmer, M. C. *Abstracts of Papers of the American Chemical Society* **2001**, *221*, U337.

(33) Henry, M. C.; Wolf, L. K.; Messmer, M. C. *Journal of Physical Chemistry B* **2003**, *107*, 2765.

(34) Henry, M. C.; Piagessi, E. A.; Zesotarski, J. C.; Messmer, M. C. *Langmuir* **2005**, *21*, 6521.

(35) Sly, K. L.; Mok, S.-W.; Conboy, J. C. *Analytical Chemistry* **2013**, *85*, 8429.